Model calibration of locally nonlinear dynamical systems: Extended constitutive relation error with multi-harmonic coefficients

Model Calibration of Locally Nonlinear Dynamical Systems: Extended Constitutive Relation Error with Multi-Harmonic Coefficients

Journal:	*Engineering Computations*
Manuscript ID	EC-10-2017-0419.R1
Manuscript Type:	Research Article
Keywords:	finite element method, ECL benchmark, constrained minimization, nonlinear model calibration, model uncertainty

1 Introduction

Local nonlinearities are pervasive in engineering applications (Shi and Atluri 1992; Fey et al. 1996; Wojtkiewicz and Johnson. 2011). In some cases, local nonlinearities are deliberately designed into the system to avoid excessively high responses or stresses (Fey 1992) and in others, they arise from large deformations or material stress (Clough and Wilson 1979). Examples include nonlinear bearings (Nelson and Nataraj 1989), dry friction damping (Ferri and Dowell 1988), local nonlinear springs and dampers (Qu 2002), structural joints with an opening and closing ability (Niwa and Clough 1982), and concrete cracking (Atamturktur et al. 2013; Llau et al. 2015).

In these systems, as the nonlinear effects are localized within a component of a larger linear system, the dynamic response tends to remain predominantly linear for small magnitude forces (Clough and Wilson 1979). However, when sufficiently high magnitude forces are applied, the dynamic behavior becomes nonlinear and is governed by the interaction between the linear and nonlinear components. Hence, when developing numerical models to represent such systems, one must pay attention to accurate modeling of both the global system that exhibits the underlying linear behavior and the spatially local component that introduces nonlinearity. It is important to note that modeling error in the underlying linear behavior could degrade the prediction accuracy of the overall nonlinear behavior, resulting in large deviations from the measured dynamic response (Lenaerts et al. 2001; Kerschen et al. 2003; Kerschen et al. 2005; Hot 2012). As such, the accuracy with which model error in local, nonlinear components can be identified is naturally dependent on errors which may be associated with linear components.

Common approaches for calibrating models of nonlinear dynamical systems can be grouped into two categories. The first category of approaches corrects errors in the representation of both the linear and nonlinear responses of the system simultaneously (Lenaerts et al. 2001; Meyer and Link 2003; Bellizzi and Defilippi 2003; Kerschen et al. 2005). These approaches may face the identifiability problem due to the large number of confounding parameters that need to be calibrated using an inevitably finite set of available measurements (Lenaerts et al. 2001; Kurt et al. 2005; Jaishi and Ren 2007; Van Buren and Atamturktur

2012). The second category of approaches, on the other hand, corrects the representation of only the nonlinear response, and therefore assumes the linear system to be modeled accurately. This assumption in turn mandates the availability of reliable *a priori* knowledge of the linear system (Kerschen et al. 2005; Isasa et al. 2011). Hence, this second approach risks that during calibration of the locally nonlinear component parameters errors in the linear system may be compensated for since the linear model accuracy is seldom guaranteed. Separately identifying the modeling errors that govern the system's linear and nonlinear behavior offers a solution that can mitigate the issues related to identifiability faced by both of these categories of approaches (Lenaerts et al. 2001; Ewins et al. 2015).

In this paper, a two-step process is presented for calibrating numerical models of dynamical systems with local nonlinearities. The process involves separately measuring the system's predominantly linear and nonlinear dynamic response under periodic excitation at low and high force magnitudes, respectively. This is a development over other published approaches that face from the previously mentioned identifiability issues. From these response measurements, multi-harmonic coefficients, a commonly used set of features for characterization of nonlinear dynamical systems (Cardona et al. 1994), are extracted. When coupled with the extended constitutive relation error (ECRE), the multi-harmonic coefficients allow the calculation of the residual energy, which reflects the discrepancy between the model predictions and the experimental measurements (Isasa et al. 2011; Hu et al. 2017). In the first step of this study, the residual energy in the predominantly linear behavior is calculated for each discretized finite element allowing us to identify the model input parameters that need calibration. These input parameters, when combined with the poorly known parameters associated with the local nonlinearity constitute the total set of calibration parameters.

Subsequently in the second step, the residual energy calculated under both the low magnitude excitation and the nonlinearity-inducing, higher magnitude excitation is minimized to update the calibration parameters. Thus, model parameter calibration becomes an optimization problem that is solved through an iterative approach combining the multi-harmonic balance method (MHB) and ECRE into a method henceforth referred to as Iterative Integrated MHB and ECRE (IIME). In this study, the performance and

efficiency of IIME are compared against discrete, sampling-based optimal value searches that are commonly used for nonlinear model calibration.

This paper is organized as follows. In Section 2, we briefly review the MHB-ECRE identification approach as applied to nonlinear dynamical systems. Section 3 describes the procedure for the two-step model calibration approach. In Section 4, the calibration approach is demonstrated on the finite element model of an academic example: a nonlinear beam with model error in both the linear and nonlinear components, using synthetically generated measurements. In this section, the efficacy of the proposed two-step approach is evaluated by comparing the obtained results against those of a one-step MHB-ECRE nonlinear model calibration. In Section 5, the limitations of the proposed approach when implemented with reduced quantity (i.e. fewer measured degrees of freedom) and quality (i.e. higher noise levels) of measurements is discussed. Moreover, the effect of the location of the excitation force and model error on the performance of the proposed method is evaluated. Finally, Section 6 draws the conclusions of this paper and summarizes the benefits and drawback of the proposed nonlinear model calibration method compared to the conventional, single-step MHB-ECRE method.

2 Background perspectives: nonlinear model calibration using the MHB-ECRE approach

When calibrating numerical models of dynamical systems, the discrepancy between model predictions and experimental measurements can be calculated using response features in modal, time, or frequency domains (Atamturktur et al. 2012). In modal domain, nonlinear effects are projected into modal space in terms of nonlinear normal modes. Nonlinear normal modes are amplitude-dependent, however, which prevents the direct separation of space and time in the governing equations of motion (Vakakis 1997; Kerschen et al. 2009). This energy dependence complicates the analytical calculation of the nonlinear normal modes, and the model calibration using nonlinear normal models often becomes computationally demanding (Kerschen et al. 2006). The use of time domain response features is less computationally demanding than modal domain features as measurement devices directly provide the desired inputs (Masri and Caughey 1979; Gondhalekar et al. 2009). Nonetheless, time domain response features are large-

dimensional and highly sensitive to measurement noise (Atamturktur and Laman 2012; Moaveni and Asgarieh 2012), which makes direct comparisons between the measurements and the model predictions in the time domain highly unreliable.

Frequency domain response features are calculated by applying a transformation process on the time domain signals to separate the response into a series of harmonics (Meyer and Link 2003; Böswald and Link 2004). In frequency domain methods, the time and space in the governing equations of motion can be easily separated through linearization using Fourier series expansion. Thus, response features in frequency domain can be expressed as a function of excitation frequency and amplitude (Ferreira and Serpa 2005). Furthermore, frequency domain features are less sensitive to noise and more compact compared to the time domain features (Kerschen et al. 2006; Atamturktur and Laman 2012). In this paper, we implement a class of frequency domain response features known as multi-harmonic coefficients calculated through the Multi-Harmonic Balance (MHB) method, chosen for their high accuracy (Ren et al. 1998) and computational efficiency (Huang et al. 2006).

2.1 Multi-harmonic balance method

The equation of motion of a nonlinear structure with local geometrical nonlinearity can be written as follows:

$$\boldsymbol{M}\ddot{\boldsymbol{x}}(t)+\boldsymbol{C}\dot{\boldsymbol{x}}(t)+\boldsymbol{K}\boldsymbol{x}(t)+K_{NL}\boldsymbol{x}^{3}(t)=\boldsymbol{p}(t) \quad (1)$$

where $\boldsymbol{M},\boldsymbol{C},\boldsymbol{K}\in\Re^{N,N}$ are the mass, damping and stiffness matrices, respectively, and N is the number of degrees of freedom (DOF) considered. The stiffness matrix is assumed to be positive definite. Here, $\boldsymbol{p}(t)$ is the external force vector and $\boldsymbol{x}(t)$ is the displacement response vector of the N DOFs at time t. In Equation (1), a spatially localized, geometrical nonlinearity is represented by the cubic stiffness, K_{NL}, multiplied by the element-wise cube of the displacement of each DOF (Worden and Tomlinson 2000).

A local, cubic nonlinearity is used in this paper as it is one of the most common cases of nonlinearity in dynamic systems (Kerschen et al. 2006; Wilson et al. 1972). It is important to note, however, the approach presented herein can be used for a wide variety of nonlinear systems (not just local nonlinearities) where

the underlying system can be analyzed and calibrated first using intentionally low excitations to the system to isolate the predominately linear behavior of the system (Stricklin and Haisler 1977).

In linear structural dynamics, the system is conveniently characterized by the structural modes and their associated resonant frequencies. In nonlinear dynamical systems, however, distinctly nonlinear features can be generated from a set of periodic response vectors. When a periodic excitation is applied to a nonlinear dynamical system, the input energy is concentrated at the excitation frequency making it relatively simple to generate nonlinear features through the transformation from time domain response into frequency domain response. This approach also yields higher signal-to-noise ratio compared to the response measured under random or transient excitations (Worden and Tomlinson 2000). Because of these benefits, solving the equation of motion of a nonlinear system under periodic excitation has become common practice for evaluating the dynamic behavior of nonlinear systems (Kerschen et al. 2006).

Most early approaches for predicting the steady-state oscillation of a nonlinear system under periodic excitation were limited to approximate calculations of the fundamental harmonic coefficients. These fundamental harmonic coefficients were assumed to have a significantly larger value compared to higher order harmonic coefficients (Stoker 1950; Tondl 1974). However, in the early 1980s, researchers began to recognize that the higher order harmonic coefficients are also essential to accurately predict the steady state response (Tamura et al. 1981; Leung and Fung 1989). To include the higher order harmonics for steady-state oscillations of a nonlinear system, Tamura et al. (1981) suggested the multi-harmonic balance (MHB) method. As an extension of the fundamental harmonic balance approach, MHB operates in the frequency domain to solve nonlinear equations of motion under periodic excitation using a Fourier series approximation. MHB has proven capability solving the periodic response of nonlinear systems more efficiently than time domain integration methods, such as Newmark's, central difference, and Runge-Kutta methods (Cardona et al. 1994).

In MHB, the periodic displacement response vector of a nonlinear system is expressed as a Fourier series:

$$\boldsymbol{x}(t) = \boldsymbol{Q}_0 + \sum_{j=1}^{n} (\boldsymbol{Q}_j^c \cos m_j \omega t + \boldsymbol{Q}_j^s \sin m_j \omega t) \tag{2}$$

where $\boldsymbol{Q}_0$ is a constant; $\boldsymbol{Q}_j^c$ and $\boldsymbol{Q}_j^s$ represent the j^{th} cosine and sine multi-harmonic coefficients, respectively; m_j is the harmonic of excitation frequency ω; and n is the number of harmonics included in the analysis. Usually, the multi-harmonic coefficients are obtained by directly applying a fast Fourier transform on the time history response of measured DOFs. If excitation frequency is constant, Fourier series and harmonic curve fitting tools can also be applied for calculating the multi-harmonic coefficients (Isasa et al. 2011).

Introducing Equation (2) into the equation of motion for the nonlinear system given in Equation (1) results in the following expression:

$$\begin{aligned} &\boldsymbol{M}\left(\sum_{j=1}^{n} (-(m_j\omega)^2 \boldsymbol{Q}_j^c \cos m_j \omega t - (m_j\omega)^2 \boldsymbol{Q}_j^s \sin m_j \omega t)\right) + \boldsymbol{C}\left(\sum_{j=1}^{n} (-m_j \omega \boldsymbol{Q}_j^c \sin m_j \omega t + m_j \omega \boldsymbol{Q}_j^s \cos m_j \omega t)\right) \\ &+\boldsymbol{K}\left(\boldsymbol{Q}_0 + \sum_{j=1}^{n} (\boldsymbol{Q}_j^c \cos m_j \omega t + \boldsymbol{Q}_j^s \sin m_j \omega t)\right) + K_{NL} \boldsymbol{x}^3(t) = \boldsymbol{p}(t) \end{aligned} \tag{3}$$

Sequentially pre-multiplying all terms in Equation (3) by the harmonic functions $(1, \cos m_1 \omega t, \sin m_1 \omega t ... \cos m_n \omega t, \sin m_n \omega t)$ and integrating from zero to the fundamental period of the system, $T = 2\pi/\omega$, the following frequency domain expression can be obtained (Isasa et al. 2011):

$$\boldsymbol{\mathcal{Z}}(\omega)\boldsymbol{Q}_\omega + \boldsymbol{F}(\boldsymbol{Q}_\omega, \omega) - \boldsymbol{P} = 0 \tag{4}$$

where $\boldsymbol{Q}_\omega = \{Q_0, Q_1, ..., Q_{2n}\}$ is the vector of harmonic coefficients with $Q_i \in \Re^{N,1}$. The matrix $\boldsymbol{\mathcal{Z}}(\omega) \in \Re^{(2n+1)N,(2n+1)N}$ is a matrix of structural system properties in the frequency domain and is expressed as:

$$\mathcal{Z}(\omega)=\begin{bmatrix} \boldsymbol{K} & 0 & 0 & \dots & 0 & 0 \\ 0 & \boldsymbol{K}-(m_1\omega)^2\boldsymbol{M} & m_1\omega\boldsymbol{C} & \dots & 0 & 0 \\ 0 & -m_1\omega\boldsymbol{C} & \boldsymbol{K}-(m_1\omega)^2\boldsymbol{M} & \dots & 0 & 0 \\ \dots & \dots & \dots & \dots & \dots & \dots \\ 0 & 0 & 0 & \dots & \boldsymbol{K}-(m_n\omega)^2\boldsymbol{M} & m_n\omega\boldsymbol{C} \\ 0 & 0 & 0 & \dots & -m_n\omega\boldsymbol{C} & \boldsymbol{K}-(m_n\omega)^2\boldsymbol{M} \end{bmatrix} \tag{5}$$

The nonlinear force vector $K_{NL}\boldsymbol{x}^3(t)$ and periodic excitation force vector $\boldsymbol{p}(t)$ in Equation (3) are also transformed from nonlinear, time domain response into linearized, frequency domain response (see Equations (6) and (7)). It is seen that each harmonic of the periodic excitation yields corresponding sine and cosine functions not only for the excitation, $\boldsymbol{P}$, but also for the force due to the localized nonlinearity, $\boldsymbol{F}(\boldsymbol{Q}_\omega,\omega)$.

Nonlinear force vectors in frequency domain $\boldsymbol{F}(\boldsymbol{Q}_\omega,\omega)\in\Re^{(2n+1)N,1}$ are then expressed as:

$$\boldsymbol{F}(\boldsymbol{Q}_\omega,\omega)=\begin{Bmatrix} \int_0^T f_{NL}(\boldsymbol{x}(t))dt \\ \frac{\omega}{\pi}\int_0^T f_{NL}(\boldsymbol{x}(t))\cos m_1\omega t dt \\ \frac{\omega}{\pi}\int_0^T f_{NL}(\boldsymbol{x}(t))\sin m_1\omega t dt \\ \vdots \\ \frac{\omega}{\pi}\int_0^T f_{NL}(\boldsymbol{x}(t))\cos m_n\omega t dt \\ \frac{\omega}{\pi}\int_0^T f_{NL}(\boldsymbol{x}(t))\sin m_n\omega t dt \end{Bmatrix} \quad \text{where } f_{NL}(\boldsymbol{x}(t))=K_{NL}\boldsymbol{x}^3(t) \tag{6}$$

Periodic excitation force vectors in frequency domain $\boldsymbol{P}\in\Re^{(2n+1)N,1}$ are expressed as:

$$\boldsymbol{P}=\begin{Bmatrix} \int_0^T \boldsymbol{p}(t)dt \\ \frac{\omega}{\pi}\int_0^T \boldsymbol{p}(t)\cos m_1\omega t dt \\ \frac{\omega}{\pi}\int_0^T \boldsymbol{p}(t)\sin m_1\omega t dt \\ \vdots \\ \frac{\omega}{\pi}\int_0^T \boldsymbol{p}(t)\cos m_n\omega t dt \\ \frac{\omega}{\pi}\int_0^T \boldsymbol{p}(t)\sin m_n\omega t dt \end{Bmatrix} \tag{7}$$

Equation (4) can be solved using the Newton–Raphson method (Ferri 1986). The number of harmonics included must be considered as it increases the size of Equation (4), and thus, increases the computation time. Models with prohibitively large linear system matrices can make use of reduction techniques (e.g. Guyan reduction) to reduce computational cost.

2.2 The integrated MHB-ECRE approach

When coupled with the extended constitutive relation error (ECRE), a method to measure the element-wise discrepancy between a model and a structure based on constitutive relations, the multi-harmonic coefficients allow the calculation of the residual energy that reflects the discrepancy between predictions and measurements (Charbonnel et al. 2013; Deraemaeker et al. 2002; Hu et al. 2017; Ladevèze and Leguillon 1983). By integrating MHB and ECRE, we seek to minimize the constitutive error of the system. This constitutive error, E_ω^2, accounts for the uncertainties in both the model predictions and the experimental measurements and is expressed as:

$$E_\omega^2 = \boldsymbol{r}_\omega^T \mathcal{K} \boldsymbol{r}_\omega + \alpha (\boldsymbol{H}\boldsymbol{Q}_\omega - \boldsymbol{Q}_\omega^e)^T \mathcal{K}_R (\boldsymbol{H}\boldsymbol{Q}_\omega - \boldsymbol{Q}_\omega^e) \tag{8}$$

where $\mathcal{K} \in \Re^{(2n+1)N,(2n+1)N}$ is the multi-harmonic stiffness matrix (Isasa et al, 2011) and is expressed as:

$$\mathcal{K} = \begin{pmatrix} \boldsymbol{K} & 0 & \cdots & 0 & 0 \\ 0 & \boldsymbol{K} & \cdots & 0 & 0 \\ \vdots & \vdots & \ddots & \vdots & \vdots \\ 0 & 0 & \cdots & \boldsymbol{K} & 0 \\ 0 & 0 & \cdots & 0 & \boldsymbol{K} \end{pmatrix} \tag{9}$$

In Equation (8), $\boldsymbol{Q}_\omega$ is the multi-harmonic coefficient vector that is expanded from experimentally identified, multi-harmonic coefficients to the total number of DOFs in the numerical model; and $\boldsymbol{Q}_\omega^e$ is the experimentally identified, multi-harmonic coefficient vector that is generated based on the experimentally measured time history response. In this study, only excitation with a constant frequency is considered; hence, $\boldsymbol{Q}_\omega^e$ is obtained using a Fourier series expansion and harmonic curve fitting. In Equation (8), $\boldsymbol{r}_\omega = \boldsymbol{Q}_\omega - \boldsymbol{V}_\omega$ is the relative multi-harmonic coefficient vector that accounts for the discrepancy between

model predictions and experimental measurements. $\boldsymbol{V}_{\omega}$ expresses the multi-harmonic coefficients obtained from model predictions. $\boldsymbol{H}$ is a transformation matrix that reduces the multi-harmonic coefficient matrix for all DOFs to the size of the measured DOFs. α is a weighting factor that accounts for the confidence level of experimental measurements (Deraemaeker et al. 2002). Finally, $\mathcal{K}_R$ is the $(2n+1)N_e \times (2n+1)N_e$ reduced multi-harmonic stiffness matrix of the numerical model obtained through Guyan model reduction (Guyan 1965), where N_e is the number of measured DOFs.

To evaluate $\boldsymbol{r}_{\omega}$ and $\boldsymbol{Q}_{\omega}$, we solve the following minimization problem:

Minimize cost function: $E_{\omega}^2 = \boldsymbol{r}_{\omega}^T \mathcal{K} \boldsymbol{r}_{\omega} + \alpha (\boldsymbol{H}\boldsymbol{Q}_{\omega} - \boldsymbol{Q}_{\omega}^e)^T \mathcal{K}_R (\boldsymbol{H}\boldsymbol{Q}_{\omega} - \boldsymbol{Q}_{\omega}^e)$ (10a)

Subjected to constraint relationship: $\mathcal{Z}(\omega)\boldsymbol{Q}_{\omega} + \boldsymbol{F}(\boldsymbol{Q}_{\omega}, \omega) - \boldsymbol{P} = \mathcal{K}\boldsymbol{r}_{\omega}$ (10b)

The constraint in Equation (10b) can be dualized using a Lagrange multiplier to form an unconstrained minimization problem.

3 Calibrating the models of nonlinear dynamical systems: Iterative Integrated MHB and ECRE (IIME)

The two-step process presented herein is conceived to identify the residual errors in the underlying linear system and those in the nonlinear component. The strategy implemented involves measuring the dynamical system vibration response under low magnitude periodic excitation such that the system vibration response is predominantly linear. Using this low magnitude excitation ($\boldsymbol{P}_1$) data, the experimental multi-harmonic coefficients ($\boldsymbol{Q}_{\omega 1}^e$) are first obtained. Next, model-predicted multi-harmonic coefficients ($\boldsymbol{V}_{\omega 1}$) are calculated and experimental multi-harmonic coefficients ($\boldsymbol{Q}_{\omega 1}$) are expanded to match the degrees of freedom of the numerical model. Through the error minimization step of ECRE, the difference between experimental multi-harmonic coefficient and model predicted multi-harmonic coefficient vectors ($\boldsymbol{Q}_{\omega 1} - \boldsymbol{V}_{\omega 1}$) is calculated. The knowledge of this disagreement, combined with the stiffness matrix, allows us to calculate the elemental residual energy. The elements with high residual energy indicate the existence of higher model error (Hu et al. 2017), and thus, the model parameters associated with these elements are

selected for calibration. This model error localization step is useful for parameter selection (Larsson and Abrahamsson 1999; Kim and Park 2004; Hu et al. 2017), because the number of parameters that need to be calibrated can often be significantly reduced in this step, which in turn helps mitigate the risk of rank deficiency and ill-conditioning during calibration (Yu et al. 2007).

In the second step, a higher magnitude periodic excitation is applied to obtain the nonlinear dynamic displacement response and the corresponding multi-harmonic coefficient is calculated ($\boldsymbol{Q}_{\omega 2}^{e}$). Using both multi-harmonic coefficients, $\boldsymbol{Q}_{\omega 1}$ and $\boldsymbol{Q}_{\omega 2}$, linear and nonlinear model parameters are calibrated by minimizing the sum of the residual energy calculated for both excitation magnitudes ($\boldsymbol{P}_1$ and $\boldsymbol{P}_2$). This way the model error in the locally nonlinear component is accurately identified all while errors in the modeling of the underlying linear system are corrected. Figure 1 schematically shows the proposed method as divided into two steps: localization and parameter calibration. The details of these two steps are given below:

Step 1. Model error localization using low magnitude excitation, $\boldsymbol{P}_1$

Based on the system response to low magnitude excitation, the optimization problem is formulated in Equation (11) that minimizes the residual energy between the numerical model and the measurements. To minimize the objective function, we formulate a saddle-point problem with the introduction of Lagrange multipliers. Equation (11) yields the system of the nonlinear equations shown in Equation (12), based on which the two unknown multi-harmonic coefficient vectors, $\boldsymbol{r}_{\omega 1}$ and $\boldsymbol{Q}_{\omega 1}$, that represent the predominantly linear dynamic response features can be solved. The relative multi-harmonic coefficient vector $\boldsymbol{r}_{\omega 1}$, combined with elemental stiffness matrix, is then used for localizing the model error in the linear component. Therefore, the linear parameters that are associated with identified model error, E_L , are selected from a large candidate set of parameters for the calibration in the next step.

Minimize the cost function for force level $\boldsymbol{P}_1$:

$$E_{\omega 1}^{2} = \boldsymbol{r}_{\omega 1}^{T} \mathcal{K} \boldsymbol{r}_{\omega 1} + \alpha (\boldsymbol{H}\boldsymbol{Q}_{\omega 1} - \boldsymbol{Q}_{\omega 1}^{e})^{T} \mathcal{K}_{R} (\boldsymbol{H}\boldsymbol{Q}_{\omega 1} - \boldsymbol{Q}_{\omega 1}^{e}) \tag{11a}$$

Subjected to constraint relationship: $\mathcal{Z}(\omega)\boldsymbol{Q}_{\omega 1} + F(\boldsymbol{Q}_{\omega 1}, \omega, K_{NL}) - \boldsymbol{P}_1 = \mathcal{K}\boldsymbol{r}_{\omega 1}$ (11b)

Nonlinear matrix equation:

$$\begin{pmatrix} \mathcal{Z}(\omega) + \dfrac{\partial \boldsymbol{F}(\boldsymbol{Q}_{\omega 1}, \omega, K_{NL})}{\partial \boldsymbol{Q}_{\omega 1}} & \alpha \boldsymbol{H}^T \mathcal{K}_R \boldsymbol{H} \\ \mathcal{K} & -\mathcal{Z}(\omega) \end{pmatrix} \begin{Bmatrix} \boldsymbol{r}_{\omega 1} \\ \boldsymbol{Q}_{\omega 1} \end{Bmatrix} + \begin{Bmatrix} 0 \\ -\boldsymbol{F}(\boldsymbol{Q}_{\omega 1}, \omega, K_{NL}) \end{Bmatrix} = \begin{Bmatrix} \alpha \boldsymbol{H}^T \mathcal{K}_R \boldsymbol{Q}^e_{\omega 1} \\ -\boldsymbol{P}_1 \end{Bmatrix} \quad (12)$$

The derivation of Equation (12) can be found by considering Equation (11a) as a saddle-point problem and applying Lagrange multipliers. The terms that compose Equation (11a) are classified as being "less reliable," namely the error in the model (first term) and the mode shape expansion error (second term) that is introduced when the experimentally measured information is extrapolated to the N model DOFs (Zimmerman and Kaouk 1994; Charbonnel et al. 2013). By subsequently applying the constraint to the optimization problem that the solution must satisfy the more reliable equilibrium equation of Equation (11b), the errors in less reliable equations can be minimized.

Step 2. Nonlinear model calibration using both low and high magnitude excitations, $\boldsymbol{P}_1$ and $\boldsymbol{P}_2$

In the second step, we combine the measurements of multi-harmonic coefficients for both low and high magnitude excitations. The sum of the residual energy for both excitation magnitudes is then minimized.

Minimize the cost function for $\boldsymbol{P}_1$ and $\boldsymbol{P}_2$:

$$\begin{aligned} E^2_{\omega\_combined} &= \boldsymbol{r}_{\omega 1}^T \mathcal{K} \boldsymbol{r}_{\omega 1} + \alpha(\boldsymbol{H}\boldsymbol{Q}_{\omega 1} - \boldsymbol{Q}^e_{\omega 1})^T \mathcal{K}_R (\boldsymbol{H}\boldsymbol{Q}_{\omega 1} - \boldsymbol{Q}^e_{\omega 1}) \\ &+ \boldsymbol{r}_{\omega 2}^T \mathcal{K} \boldsymbol{r}_{\omega 2} + \alpha(\boldsymbol{H}\boldsymbol{Q}_{\omega 2} - \boldsymbol{Q}^e_{\omega 2})^T \mathcal{K}_R (\boldsymbol{H}\boldsymbol{Q}_{\omega 2} - \boldsymbol{Q}^e_{\omega 2}) \end{aligned} \quad (13a)$$

Subjected to the following constraints:

$$\mathcal{Z}(\omega)\boldsymbol{Q}_{\omega 1} + \boldsymbol{F}(\boldsymbol{Q}_{\omega 1}, \omega, K_{NL}) - \boldsymbol{P}_1 = \mathcal{K}\boldsymbol{r}_{\omega 1} \quad (13b)$$

$$\mathcal{Z}(\omega)\boldsymbol{Q}_{\omega 2} + \boldsymbol{F}(\boldsymbol{Q}_{\omega 2}, \omega, K_{NL}) - \boldsymbol{P}_2 = \mathcal{K}\boldsymbol{r}_{\omega 2} \quad (13c)$$

A new cost function g_c is obtained after applying the Lagrange multipliers and is expressed as follows:

$$\begin{aligned} g_c &= \boldsymbol{r}_{\omega 1}^T \mathcal{K} \boldsymbol{r}_{\omega 1} + \alpha(\boldsymbol{H}\boldsymbol{Q}_{\omega 1} - \boldsymbol{Q}^e_{\omega 1})^T \mathcal{K}_R (\boldsymbol{H}\boldsymbol{Q}_{\omega 1} - \boldsymbol{Q}^e_{\omega 1}) + \psi_1^T (\mathcal{K}\boldsymbol{r}_{\omega 1} - \mathcal{Z}(\omega)\boldsymbol{Q}_{\omega 1} - \boldsymbol{F}(\boldsymbol{Q}_{\omega 1}, \omega, K_{NL}) + \boldsymbol{P}_1) \\ &+ \boldsymbol{r}_{\omega 2}^T \mathcal{K} \boldsymbol{r}_{\omega 2} + \alpha(\boldsymbol{H}\boldsymbol{Q}_{\omega 2} - \boldsymbol{Q}^e_{\omega 2})^T \mathcal{K}_R (\boldsymbol{H}\boldsymbol{Q}_{\omega 2} - \boldsymbol{Q}^e_{\omega 2}) + \psi_2^T (\mathcal{K}\boldsymbol{r}_{\omega 2} - \mathcal{Z}(\omega)\boldsymbol{Q}_{\omega 2} - \boldsymbol{F}(\boldsymbol{Q}_{\omega 2}, \omega, K_{NL}) + \boldsymbol{P}_2) \end{aligned} \quad (14)$$

where ψ_1 and ψ_2 are the Lagrange multipliers for the constraint relationships for $\boldsymbol{P}_1$ and $\boldsymbol{P}_2$, respectively. Through the calculation of the stationary conditions of g_c with respect to the unknowns $\boldsymbol{r}_{\omega 1}$, $\boldsymbol{Q}_{\omega 1}$, $\boldsymbol{r}_{\omega 2}$, $\boldsymbol{Q}_{\omega 2}$, E_L, K_{NL}, ψ_1, and ψ_2, the solution of Equation (14) is calculated using the following matrix relationship:

$$\begin{bmatrix} \mathcal{Z}(\omega)+\dfrac{\partial \boldsymbol{F}(\boldsymbol{Q}_{\omega 1},\omega,K_{NL})}{\partial \boldsymbol{Q}_{\omega 1}} & \alpha \boldsymbol{H}^T \mathcal{K}_R \boldsymbol{H} & 0 & 0 & 0 & 0 \\ \mathcal{K} & -\mathcal{Z}(\omega) & 0 & 0 & 0 & 0 \\ 0 & 0 & \mathcal{Z}(\omega)+\dfrac{\partial \boldsymbol{F}(\boldsymbol{Q}_{\omega 2},\omega,K_{NL})}{\partial \boldsymbol{Q}_{\omega 2}} & \alpha \boldsymbol{H}^T \mathcal{K}_R \boldsymbol{H} & 0 & 0 \\ 0 & 0 & \mathcal{K} & -\mathcal{Z}(\omega) & 0 & 0 \\ 0 & 0 & 0 & 0 & 0 & 0 \\ 0 & 0 & 0 & 0 & 0 & 0 \end{bmatrix} \begin{Bmatrix} \boldsymbol{r}_{\omega 1} \\ \boldsymbol{Q}_{\omega 1} \\ \boldsymbol{r}_{\omega 2} \\ \boldsymbol{Q}_{\omega 2} \\ E_L \\ K_{NL} \end{Bmatrix} + \begin{Bmatrix} 0 \\ -\boldsymbol{F}(\boldsymbol{Q}_{\omega 1},\omega,K_{NL}) \\ 0 \\ -\boldsymbol{F}(\boldsymbol{Q}_{\omega 2},\omega,K_{NL}) \\ \dfrac{\partial g}{\partial E_L} \\ \dfrac{\partial g}{\partial K_{NL}} \end{Bmatrix} = \begin{Bmatrix} \alpha \boldsymbol{H}^T \mathcal{K}_R \boldsymbol{Q}^e_{\omega 1} \\ -\boldsymbol{P}_1 \\ \alpha \boldsymbol{H}^T \mathcal{K}_R \boldsymbol{Q}^e_{\omega 2} \\ -\boldsymbol{P}_2 \\ 0 \\ 0 \end{Bmatrix} \tag{15}$$

where E_L are the linear structural parameters corresponding to the identified model error in the linear component.

All the above objective functions are convex, thus facilitating the use of efficient local optimization algorithms in the calibration process. A modified Newton-Raphson algorithm is chosen to solve this nonlinear problem due to its desirable convergence characteristics (Nocedal and Wright 2006; Stevens et al. 2017) and because the parameter gradients are calculated numerically. In each of the Newton-Raphson iterations, the parameters are calibrated and the residual error term is recalculated. A new iteration consisting of a localization step and a correction step is performed until the prescribed convergence criterion is satisfied.

Instead of iteratively calibrating the parameters corresponding to linear and nonlinear behavior (i.e. using IIME), calibration can also be conducted based on a discrete set of inputs−henceforth referred to as

Discrete Integrated MHB-ECRE (DIME). In the DIME approach, a sample set of values are generated for the poorly-known model input parameters and then used for calculation of the residual energy using Equation (13) and (14). As such, the minimum residual energy is expected to be achieved when the calibration parameters associated with the linear and nonlinear components are closest to the true parameter values. In DIME, a large number of instances must be calculated, which means the discrete approach is more computationally demanding than IIME. In the following section, the results obtained with the DIME approach are used as a reference to compare against those obtained with the proposed two-step IIME approach.

4 Benchmark beam model application

4.1 The description of the numerical model

The proposed approach is demonstrated on a simulated academic example based on the COST action F3 project benchmark structure developed at Ecole Centrale de Lyon (Thouverez 2003; Worden 2003). The model consists of a main beam clamped to a thin, secondary beam with both ends of the structure clamped to fixed supports (see Figure 2). The main beam has a length of 0.7 m and a thickness of 0.014 m, whereas the secondary beam has a length of 0.04 m with a thickness of $5\text{x}10^{-4}$ m. Both beams have a width of 0.014 m and are comprised of steel with a Young's modulus of 210 GPa and a Poisson's ratio of 0.33. Table 1 lists the reference configuration of the F3 project benchmark model. The main beam is modeled with seven elements and the secondary beam with four elements as shown in Figure 2. The connection of the beams is modeled by a semi-rigid, rotational spring and a grounded, translational spring element with cubic stiffness such that the nodes are constrained to have the same translation displacement, but allowed to have different rotations. The value of the cubic stiffness (K_{NL}) is set to be 6.1×10^{9} N/m.

Vibration response measurements are synthetically generated for 21 DOFs along the beam as shown in Figure 3. For the low magnitude excitation, a stepped sine force with a magnitude of 0.5 N and frequency of 32 Hz, selected based on the value of the fundamental frequency of the linear beam, is applied to the structure. For the high magnitude excitation, a stepped sine force with a magnitude of 5 N and

frequency of 32 Hz is applied to ensure sufficiently large deflections to observe the nonlinear dynamic effects. In addition, simulated measurement noise is introduced as an additive zero mean Gaussian white noise at a level of 5% of the maximum displacement time history response. The noise is added to the time history measurements before the experimental multi-harmonic coefficients vectors are calculated.

The initial model is preset to have error in two distinct forms (recall Figure 2): (i) model error in the linear beam structure that is simulated by intentionally reducing the Young's modulus for element 3 by 50% (i.e. 105 GPa); (ii) model error in the nonlinear spring that is simulated by intentionally altering the stiffness coefficient with cubic nonlinearity by 50% (i.e. 3.05×10^9 N/m).

4.2 The conventional approach: MHB-ECRE using only high magnitude excitation

This section presents the results of the conventional, one-step MHB-ECRE approach in which the parameter of the nonlinear translational stiffness (K_{NL}) is calibrated with the presumption that the model of the underlying linear system is error-free. The effect of the model error in the linear beam on the results of this conventional approach is evaluated using both a model with and without the manually introduced reduction in the Young's modulus of element 3.

Owing to the need that the structure's dynamic response must exhibit nonlinear behavior for the one-step MHB-ECRE method, synthetic response measurements are generated by the model under the high amplitude excitation (5 N), using which the ECRE values are calculated by solving Equation (11).

Figure 4 depicts the ECRE values obtained for a range of nonlinear stiffness values where the correction coefficient that multiplies the nonlinear stiffness parameter (K_{NL}) varies from 0.5 to 1.5 with an interval of 0.1, essentially representing a correction of 50% below and above the nominal stiffness value. For this given range of nonlinear stiffness coefficients, the residual energy is calculated using both the 'exact' linear model (the solid curve in Figure 4) and the 'erroneous' linear model (i.e. one with a reduced Young's modulus in element 3; the dashed curve in Figure 4). The results shown in Figure 4 indicate that the linear model error leads to a 30% deviation from the true value for the identified nonlinear stiffness parameter. This difference is due to the fact that the ECRE values are biased by the model error present in the linear component and thus, the minima no longer corresponds to the *true* value of the nonlinear stiffness.

4.3 The two-step approach: MHB-ECRE using two excitation magnitudes

In this section, the proposed, iterative, two-step approach is used to calibrate the model input parameters of both the Young's modulus of element 3 and the nonlinear stiffness (K_{NL}) and verify its ability to accurately calibrate the parameters without suffering the confounding effects of error in both the linear and nonlinear components of the structure. The efficiency of this iterative approach in its search algorithm to find the optimal input parameters is compared to the discrete (DIME) approach which tests over a grid sampling of possible parameters.

The structure is excited at node 3 using the lower amplitude periodic force (0.5N) to obtain the synthetic structural vibration response with negligible nonlinear effects. As shown in Figure 5 (a), the nonlinear effects lead to only a 1.5% shift in the fundamental frequency of the structural system, while no significant distortion can be observed in the Frequency Response Function (FRF) of the nonlinear beam model with respect to the linear model. Hence, the obtained dynamic response is predominantly linear. The ECRE calculated for all beam elements is shown in Figure 6. From the figure, element 3 (E_L) is identified with the highest ECRE value, which is consistent with the fact that an incorrect Young's modulus value is assigned for this element.

The structure is then excited at the same location using the higher amplitude periodic excitation (5N) to observe the synthetic nonlinear vibration. The FRF of the translational DOF associated with the nonlinear spring is presented in Figure 5 (b). A significant distortion of 12.5% in the FRF plots is observed where the peaks shift from 32 to 36 Hz under high magnitude excitation, confirming that a sufficiently high force is applied to observe the nonlinear response.

Both IIME and DIME approaches are used to calibrate the selected model parameters as presented in the Figure 7. The IIME approach is applied by solving Equation (15) using the Newton-Raphson algorithm. The convergence threshold for the IIME approach is set to 10^{-10} for the norm of the relative solution vector between iterations. In Figure 7, it is noticed that the IIME approach is completed within 5 iterations. The calibrated linear and nonlinear model parameters are 210.21 GPa and 6.08×10^{9} N/m, respectively, which represent a 0.1% and 0.4% deviation from the true values, respectively. The detailed

calibration results for each iteration are also provided in Table 2. For the DIME approach, a range of coefficients that multiply the nonlinear stiffness (K_{NL}) and Young's modulus in the linear component (E_L) is created from 50% to 150% of the true value with an interval of 10%. These pre-defined sets of model parameters are substituted into Equation (15) and a surface plot of the residual energy is shown in Figure 7. The detailed calibration results for each iteration are also provided in Table 2.

5 Discussions on the performance of proposed method

In this section, the impact of measurement noise, number of response measurement locations, and model error location on the accuracy of the proposed method is examined. The purpose of conducting these studies is to evaluate the proposed approach's robustness and to understand how the method performs under a variety of realistic scenarios. All the calibration results presented in this section are obtained using an identical procedure as detailed in Section 4.

5.1 Model calibration considering varying noise levels

All practical experimental data is inevitably contaminated by noise to some degree (Modak et al. 2002). To assess the impact of measurement noise, in this section, the performance of the proposed model calibration method is evaluated in the presence of varying levels of noise. Accordingly, the two-step model calibration process is applied in the presence of zero mean Gaussian white noise with varying standard deviations of 5%, 10%, 15%, and 20%. For each noise level, 10 random realizations of noise are generated to contaminate the time history data and the calibrated model parameters are obtained using these contaminated measurements.

The mean and standard deviation for the calibrated stiffness coefficients for these ten realizations are shown in Figure 8. The solid line in Figure 8 shows that the linear stiffness parameter is estimated with less than 1% deviation from the true value when the noise level is less than 15%. With 20% noise, the calibrated linear stiffness parameter deviates by 5.6%. The calibrated nonlinear stiffness parameter is observed to be more sensitive to the measurement noise. The dashed line in Figure 8 shows that the nonlinear stiffness parameter is accurately estimated with less than 1% deviation when the noise level is

less than 10%. As the noise level increases to 15% and 20%, the calibrated nonlinear stiffness parameter deviates by 6.1% and 11.2%, respectively.

5.2 Model calibration with reduced set of measurements

In practical application, the number of measured response locations is limited by the feasible number of sensors, measurement channels available, and the inaccessibility of some measurement locations (Majumder and Manohar 2003). To assess the effect of such limitations, this section evaluates he performance of the proposed two-step model calibration approach by hypothetically reducing the set of measured DOFs. Three reduced sets of measurements are used to obtain the multi-harmonic coefficient vectors as shown in Figure 9. The first two measurements are with 10 (Figure 9 (a)) and 5 (Figure 9 (b)) translational DOFs including the DOF at the nonlinear spring, while the last set of measurements is with 5 (Figure 9 (c)) translational DOFs excluding the DOF at the nonlinear component. Using the reduced set of measurements, the residual energy plot for model error localization is shown in Figure 10.

As seen in Figure 11, the calibrated values for the nonlinear stiffness coefficient match the true parameter values even when the number of measurements is as low as 5 DOFs. The value of the parameter associated with the linear element with error is correctly calibrated with 10 measured DOFs, while an 8% deviation from the true values is present when only 5 DOFs are measured. When the DOF at the nonlinear spring is not included in the measurement, Figure 12 shows that the linear calibrated stiffness coefficient has a 12.3% deviation from the true value, and the nonlinear calibrated stiffness coefficient has a 26.1% deviation from the true value. The calibration of the nonlinear stiffness coefficient parameter is less affected by a reduced set of measurements as long as the response associated with the nonlinear spring is measured. It is concluded that it is important to measure the response as close to where local nonlinearity is present as possible to ensure the accuracy of the results of the proposed model calibration method.

5.3 The effect of model error location

The objective of this section is to investigate the effect the spatial distribution of modeling error on the linear system on the obtained results for the calibrated model. Specifically, we introduced model error

to 7 different elements (elements 1 to 7) of the main beam, simulated by reducing the Young's modulus by 50%. The model error in the nonlinear component is kept the same as defined in Section 4 for the seven sets of calibration cases. The proposed approach is applied to calibrate the linear and nonlinear structural component parameters, and the calibration results are plotted in Figure 13 (a) and (b), respectively. As shown in the Figure 13 (a) and (b), the convergence rate to the true value for the linear and nonlinear stiffness parameters is similar (five iterations) for all seven cases regardless of the model error location.

5.4 The effect of excitation force location

In this section, the effect of the location of the excitation force, and thus the distance between the applied force location and nonlinear spring component on the performance of model calibration results is evaluated (see Figure 14). Similar to the calibration results presented in Section 5.3, the unknown structural parameters mostly converge to the true value with the proposed calibration approach. The calibration results for all seven force locations are presented in Figure 13 (c) and (d). Figure 13 (c) shows that the averaged calibrated nonlinear stiffness coefficient relative to the true value for different locations is 0.9992 with a standard deviation of 0.0029.

Compared to the calibration of the nonlinear structural parameter, the average calibrated linear stiffness coefficient is 1.0232, which deviates slightly from the true parameter value (see Figure 13 (d)). Also, a larger standard deviation of 0.0362 is observed relative to the nonlinear stiffness calibration. Moreover, it can be concluded from Figure 13 (b) and (d) that the calibration of linear model parameters is affected by the location of the excitation force relative to the location of the model error. As the excitation force moves from the left end of the beam to the right end, the calibrated linear parameters deviate more from the true parameter value. This effect may be because as the magnitude of response becomes larger as the distance between force location and nonlinear spring element decreases, the total response is more likely to be dominated by the nonlinear effect. Thus, the accuracy of the linear parameter calibration results is influenced.

6 Conclusion

This paper presents a two-step, nonlinear model calibration framework referred to as IIME that simultaneously corrects modeling error in both linear and nonlinear components based on the combined MHB-ECRE algorithm. An appealing feature of this approach is that modeling errors in the underlying linear model can be isolated and corrected, reducing their degrading effects in the model calibration of the nonlinear component. For this, the modeling errors in the linear system are localized by applying low magnitude excitation that ensures the dynamic response of the system remains predominantly linear. Accordingly, subsequent optimization step for parameter calibration is formulated to determine both the parameters associated with poorly modeled linear components and those associated with the nonlinear components without making any assumptions regarding initial linear model accuracy.

The proposed method has been demonstrated on a numerical example (the F3 project benchmark structure) using synthetic measurements. The results show that the Integrated MHB-ECRE method is capable of calibrating nonlinear models with model error in both linear and nonlinear components. When model error is present in both linear and nonlinear components, this two-step integrated MHB-ECRE calibration approach has shown superiority to the conventional one-step MHB-ECRE approach of previous literature, while providing more reliable calibration of the nonlinear component parameter with less dependency on *a priori* knowledge of the accuracy of the associated linear system. An iterative optimization process is developed for solving the calibration problem so that the model parameters can be calibrated with less computational cost and more accurate results compared to a discretized approach.

Work has also been conducted to quantify the influence of measurement noise, a reduced set of measurements, and model error location on the proposed method. These studies show that the method is quite robust against introduced measurement noise, especially in the calibration of the linear component parameter to the true value. In addition, as long as the structural response is measured close to the location of the nonlinearity, the method has shown calibration capability with a relatively scarce set of measured data points. The proposed method has been evaluated for a case that entails a spatially localized nonlinearity, there is room for further work in testing the approach in calibrating other types of nonlinearity,

such as nonlinear material properties. One area for further work includes the natural extension of this approach in increasing the applied excitation in a gradual manner and assessing the residual energy between model predictions and the experimental measurements. This extension would expand the proposed approach from a "two-step" method to an iterative, multi-step approach. The authors believe that complicated systems could benefit from this iterative series of increasing excitations to gradually improve the predominately linear and then nonlinear model accuracy if the two responses cannot be clearly distinguished from one another with a single excitation step. This is certainly an area of further research in the development of a more universally-applicable framework for nonlinear system identification and calibration.

References

Atamturktur, S., Gilligan, C., & Salyards, K. (2013). Detection of Internal Defects in Concrete Members Using Global Vibration Characteristics. *Materials Journal (ACI)*, *110*(5), 529-538.

Atamturktur, S., Hemez, F., & Laman, J. (2012). Uncertainty Quantification in Model Verification and Validation as Applied to Large Scale Historic Masonry Monuments. *Engineering Structures (Elsevier)*, *43*, 221-234.

Atamturktur, S. & Laman, J. (2012). Finite Element Model Correlation and Calibration of Historic Monuments: Review. *Journal of Structural Design of Tall and Special Buildings (Wiley)*, *21*(2), 96-113.

Bellizzi, S., & Defilippi, M. (2003). Non-linear mechanical systems identification using linear systems with random parameters. *Mechanical Systems and Signal Processing*, *17*(1), 203-210.

Böswald, M., & Link, M. (2004). Identification of non-linear joint parameters by using frequency response residuals. *In Proceedings of the 2004 International Conference on Noise and Vibration Engineering (ISMA2004), Leuven, Belgium, September*, 20-22.

Cardona, A., Coune, T., Lerusse, A., & Geradin, M. (1994). A multiharmonic method for non-linear vibration analysis. *International Journal for Numerical Methods in Engineering*, *37*(9), 1593-1608.

Charbonnel, P. E., Ladevèze, P., Louf, F., & Le Noac'h, C. (2013). A robust CRE-based approach for model updating using in situ measurements. *Computers & Structures*, *129*, 63-73.

Clough, R. W., & Wilson, E. L. (1979). Dynamic analysis of large structural systems with local nonlinearities. *Computer Methods in Applied Mechanics and Engineering*, *17*, 107-129.

Deraemaeker, A., Ladevèze, P., & Leconte, P. (2002). Reduced bases for model updating in structural dynamics based on constitutive relation error. *Computer Methods in Applied Mechanics and Engineering*, *191*(21), 2427-2444.

Ewins, D. J., Weekes, B., & Delli Carri, A. (2015). Modal testing for model validation of structures with discrete nonlinearities. *Philosophical Transactions of the Royal Society A*, *373*(2051), 20140410.

Ferreira, J. V., & Serpa, A. L. (2005). Application of the arc-length method in nonlinear frequency response. *Journal of Sound and Vibration*, *284*(1), 133-149.

Ferri, A. A. (1986). On the equivalence of the incremental harmonic balance method and the harmonic balance-Newton Raphson method. *Journal of Applied Mechanics*, *53*(2), 455-457.

Ferri, A. A., & Dowell, E. H. (1988). Frequency domain solutions to multi-degree-of-freedom, dry friction damped systems. *Journal of Sound and Vibration*, *124*(2), 207-224.

Fey, R. H. B, Van Campen, D. H., & De Kraker, A. (1996). Long term structural dynamics of mechanical systems with local nonlinearities. *Journal of Vibration and Acoustics*, *118*, 147-153.

Fey, R. H. B. (1992). Steady-state behaviour of reduced dynamic systems with local nonlinearities. *Technische Universiteit Eindhoven*.

Gondhalekar, A. C., Petrov, E. P., & Imregun, M. (2009). Parameters identification for nonlinear dynamic systems via genetic algorithm optimization. *Journal of Computational and Nonlinear Dynamics*, *4*(4), 041002.

Guyan, R. J. (1965). Reduction of stiffness and mass matrices. *AIAA Journal*, *3*(2), 380.

Hot, A. (2012). *Validation expérimentale de structures localement non-linéaires dans un contexte spatial* (Doctoral dissertation, Besançon).

Hu, X., Prabhu, S., Atamturktur, S., & Cogan, S. (2017). Mechanistically-informed damage detection using dynamic measurements: Extended constitutive relation error. *Mechanical Systems and Signal Processing*, *85*, 312-328.

Huang, S., Petrov, E. P., & Ewins, D. J. (2006). Comprehensive analysis of periodic regimes of forced vibration for structures with nonlinear snap-through springs. *Applied Mechanics and Materials*, *5*(6) 3-13.

Isasa, I., Hot, A., Cogan, S., & Sadoulet-Reboul, E. (2011). Model updating of locally non-linear systems based on multi-harmonic extended constitutive relation error. *Mechanical Systems and Signal Processing*, *25*(7), 2413-2425.

Jaishi, B., & Ren, W. X. (2007). Finite element model updating based on eigenvalue and strain energy residuals using multiobjective optimisation technique. *Mechanical Systems and Signal Processing*, *21*(5), 2295-2317.

Kerschen, G., Golinval, J. C., Vakakis, A. F., & Bergman, L. A. (2005). The method of proper orthogonal decomposition for dynamical characterization and order reduction of mechanical systems: an overview. *Nonlinear Dynamics*, *41*(1-3), 147-169.

Kerschen, G., Lenaerts, V., & Golinval, J. C. (2003). Identification of a continuous structure with a geometrical non-linearity. Part I: Conditioned reverse path method. *Journal of Sound and Vibration*, *262*(4), 889-906.

Kerschen, G., Worden, K., Vakakis, A. F., & Golinval, J. C. (2006). Past, present and future of nonlinear system identification in structural dynamics. *Mechanical Systems and Signal Processing*, *20*(3), 505-592.

Kerschen, G., Peeters, M., Golinval, J. C., & Vakakis, A. F. (2009). Nonlinear normal modes, Part I: A useful framework for the structural dynamicist. *Mechanical Systems and Signal Processing*, *23*(1), 170-194.

Kim, G. H., & Park, Y. S. (2004). An improved updating parameter selection method and finite element model update using multiobjective optimisation technique. *Mechanical Systems and Signal Processing*, *18*(1), 59-78.

Kurt, M., Eriten, M., McFarland, D. M., Bergman, L. A., & Vakakis, A. F. (2015). Methodology for model updating of mechanical components with local nonlinearities. *Journal of Sound and Vibration*, *357*, 331-348.

Ladevèze, P. & Leguillon, D. (1983). Error Estimate Procedure in the Finite Element Method and Applications. *SIAM J. Numer. Anal.*, *20*(3), 485-509.

Larsson, A., & Abrahamsson, T. (1999). A comparison of finite element model error localization methods. In *IMAC XVII-17th International Modal Analysis Conference-Modal Analysis: Reducing the Time to Market*, 929-935.

Lenaerts, V., Kerschen, G., & Golinval, J. C. (2001). Proper orthogonal decomposition for model updating of non-linear mechanical systems. *Mechanical Systems and Signal Processing*, *15*(1), 31-43.

Leung, A. Y. T., & Fung, T. C. (1989). Phase increment analysis of damped Duffing oscillators. *International Journal for Numerical Methods in Engineering*, *28*(1), 193-209.

Llau, A., Jason, L., Dufour, F., & Baroth, J. (2015). Adaptive zooming method for the analysis of large structures with localized nonlinearities. *Finite Elements in Analysis and Design*, *106*, 73-84.

Majumder, L., Manohar, C.S. (2003). A time-domain approach for damage detection in beam structures using vibration data with a moving oscillator as an excitation source. *Journal of Sound and Vibration*, *268*(6), 699-716.

Masri, S. F., & Caughey, T. (1979). A nonparametric identification technique for nonlinear dynamic problems. *Journal of Applied Mechanics*, *46*(2), 433-447.

Meyer, S., & Link, M. (2003). Modelling and updating of local non-linearities using frequency response residuals. *Mechanical Systems and Signal Processing*, *17*(1), 219-226.

Moaveni, B., & Asgarieh, E. (2012). Deterministic-stochastic subspace identification method for identification of nonlinear structures as time-varying linear systems. *Mechanical Systems and Signal Processing*, *31*, 40-55.

Nelson, H. D., & Nataraj, C. (1989). Periodic solutions in rotor dynamic systems with nonlinear supports: a general approach. *Journal of Vibration, Acoustics, Stress and Reliability in Design*, *111*, 187-193.

Niwa, A., & Clough, R. W. (1982). Non-linear seismic response of arch dams. *Earthquake Engineering & Structural Dynamics*, *10*(2), 267-281.

Nocedal, J., & Wright, S. (2006). *Numerical optimization*. Springer Science & Business Media.

Qu, Z. Q. (2002). Model reduction for dynamical systems with local nonlinearities. *AIAA Journal*, *40*(2), 327-333.

Ren, Y., Lim, T. M., & Lim, M. K. (1998). Identification of properties of nonlinear joints using dynamic test data. *Transactions-ASME, Journal of Vibration and Acoustics*, *120*, 324-330.

Schultze, J. F., Hemez, F. M., Doebling, S. W., & Sohn, H. (2001). Application of non-linear system model updating using feature extraction and parameter effects analysis. *Shock and Vibration*, *8*(6), 325-337.

Shi, G., & Atluri, S. N. (1992). Nonlinear dynamic response of frame-type structures with hysteretic damping at the joints. *AIAA Journal*, *30*(1), 234-240.

Stevens, G., Atamturktur, S., Lebensohn, R., & Kaschner, G. (2016). Experiment-based validation and uncertainty quantification of coupled multi-scale plasticity models. *Multidiscipline Modeling in Materials and Structures*, *12*(1), 151-176.

Stoker, J. J. (1950). *Nonlinear vibrations in mechanical and electrical systems*. New York: Interscience Publishers.

Stricklin, J. A. & Haisler, W. E. (1977). Formulations and solution procedures for nonlinear structural analysis. *Computers & Structures*, 7, 125-136.

Tamura, H., Tsuda, Y., & Sueoka, A. (1981). Higher approximation of steady oscillations in nonlinear systems with single degree of freedom: Suggested multi-harmonic balance method. *Bulletin of JSME*, *24*(195), 1616-1625.

Thouverez, F. (2003). Presentation of the ECL benchmark. *Mechanical Systems and Signal Processing*, *17*(1), 195-202.

Tondl, A. (1974). Notes on the solution of forced oscillations of a third-order non-linear system. *Journal of Sound and Vibration*, *37*(2), 273-279.

Vakakis, A. F. (1997). Non-linear normal modes (NNMs) and their applications in vibration theory: an overview. *Mechanical Systems and Signal Processing*, *11*(1), 3-22.

Van Buren, K. & Atamturktur, S. (2012). A Comparative Study: Predictive Modeling of Wind Turbine Blades. *Journal of Wind Engineering*, 36(3), 235- 250.

Wilson, E. L., Farhoomand, I., & Bathe, K. J. (1972). Nonlinear dynamic analysis of complex structures. *Earthquake Engineering & Structural Dynamics*, *1*(3), 241-252.

Wojtkiewicz, S. F., & Johnson, E. A. (2011). Efficient uncertainty quantification of dynamical systems with local nonlinearities and uncertainties. *Probabilistic Engineering Mechanics*, *26*(4), 561-569.

Worden, K. (2003). Cost action F3 on structural dynamics: benchmarks for working group 2—structural health monitoring. *Mechanical systems and signal processing*, *17*(1), 73-75.

Worden, K., & Tomlinson, G. R. (2000). *Nonlinearity in structural dynamics: detection, identification and modelling*. CRC Press.

Yu, E., Taciroglu, E., & Wallace, J. W. (2007). Parameter identification of framed structures using an improved finite element model-updating method—Part I: formulation and verification. *Earthquake Engineering & Structural Dynamics*, *36*(5), 619-639.

Zimmerman, D.C. & Kaouk, M. (1994). Structural damage detection using minimum rank update theory. *J. Vib. Acoust.*, *116*(2), 222-231.

Table 1. Reference configuration of the benchmark beam model

Symbol	Parameter	Value
L_1	Length of Main Beam	0.7 m
L_2	Length of Thin Beam	0.04m
b	Width of Cross Section	0.14 m
h_1	Height of Main Beam	0.14 m
h_2	Height of Thin Beam	0.0005 m
ρ	Density	7830 kg/m^3
E	Young's modulus	210 GPa
ν	Poisson's ratio	0.33
N_{node}	Node Number	12
N_{dof}	DOF Number	21
N_e	Beam Element Number	11
N_m	Measured Dofs	21

Table 2. Model calibration results using IIME approach

Iteration number	Calibrated linear parameter (GPa)	Percentage error	Calibrated nonlinear parameter (N/m)	Percentage error	ECRE
0	105	-50.00%	3.05×10^{9}	-50.00%	1.81×10^{-5}
1	159.18	-24.20%	4.28×10^{9}	-29.80%	3.50×10^{-5}
2	182.28	-13.20%	4.98×10^{9}	-18.30%	7.91×10^{-6}
3	223.86	6.60%	6.80×10^{9}	11.50%	4.40×10^{-6}
4	210.21	0.10%	5.99×10^{9}	-1.80%	5.18×10^{-7}
5	210.21	0.10%	6.08×10^{9}	-0.40%	4.34×10^{-7}

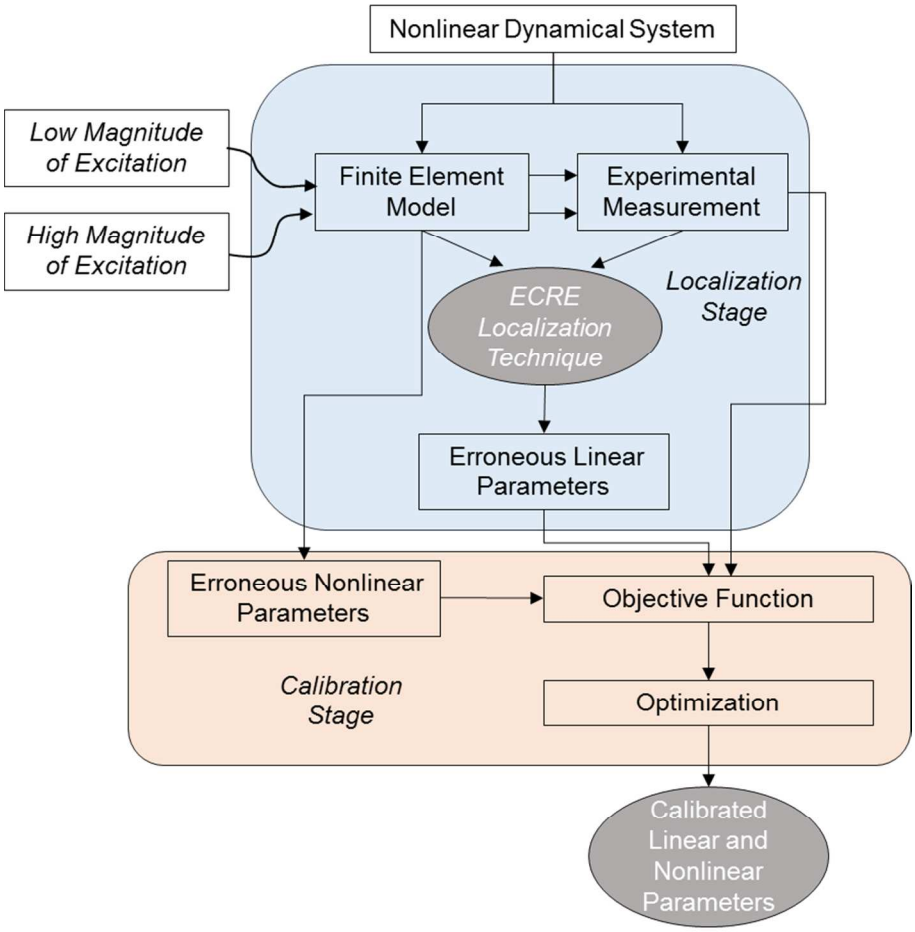

Figure 1. The calibration procedure for the proposed method

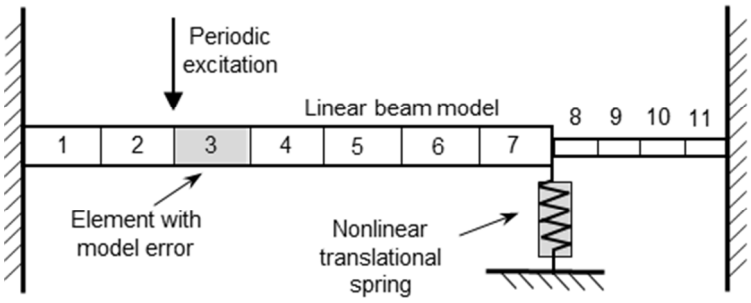

Figure 2. A linear beam model with local nonlinearity under periodic excitation

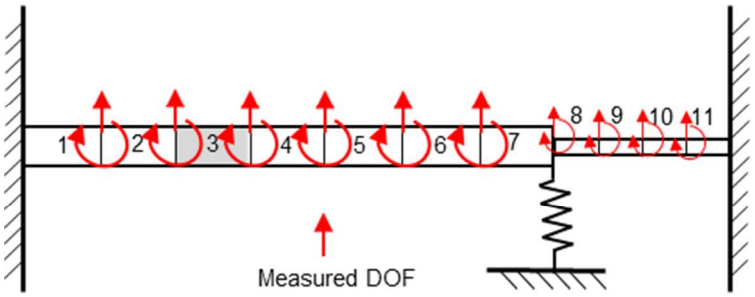

Figure 3. The experimentally measured translational and rotational DOFs

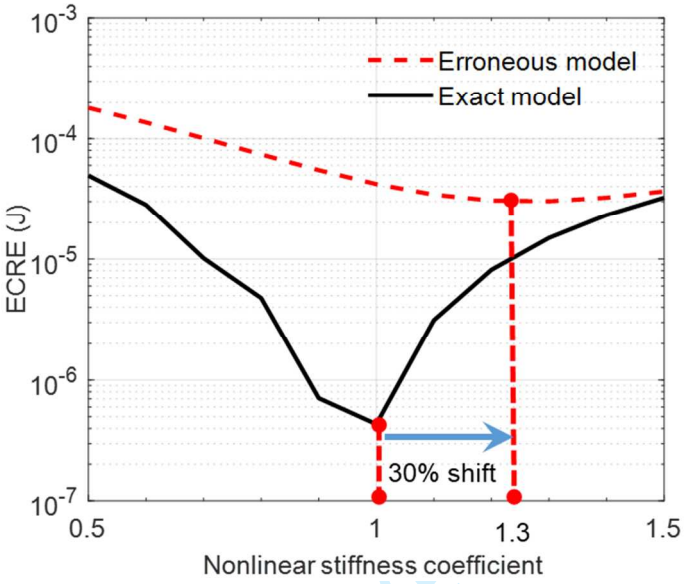

Figure 4. Nonlinear parameter identification result when the linear stiffness coefficient is 0.5 and 1

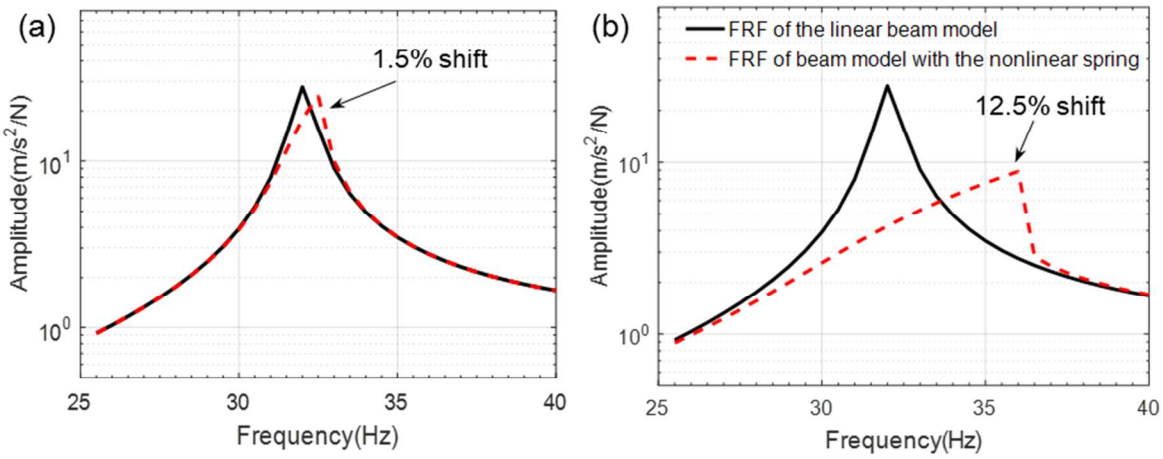

Figure 5. Comparison of FRFs at node 8 for the linear beam model with and without the nonlinear spring: (a) a low magnitude excitation of 0.5 N is applied; (b) a high magnitude excitation of 5 N is applied

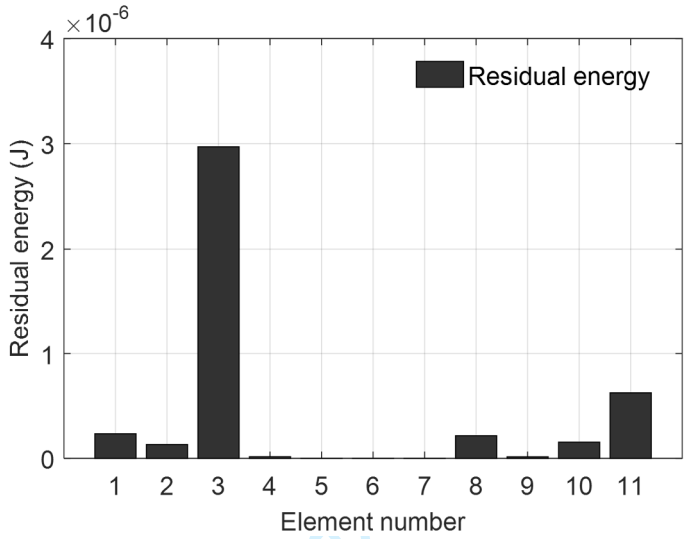

Figure 6. The ECRE localization of model error in linear component

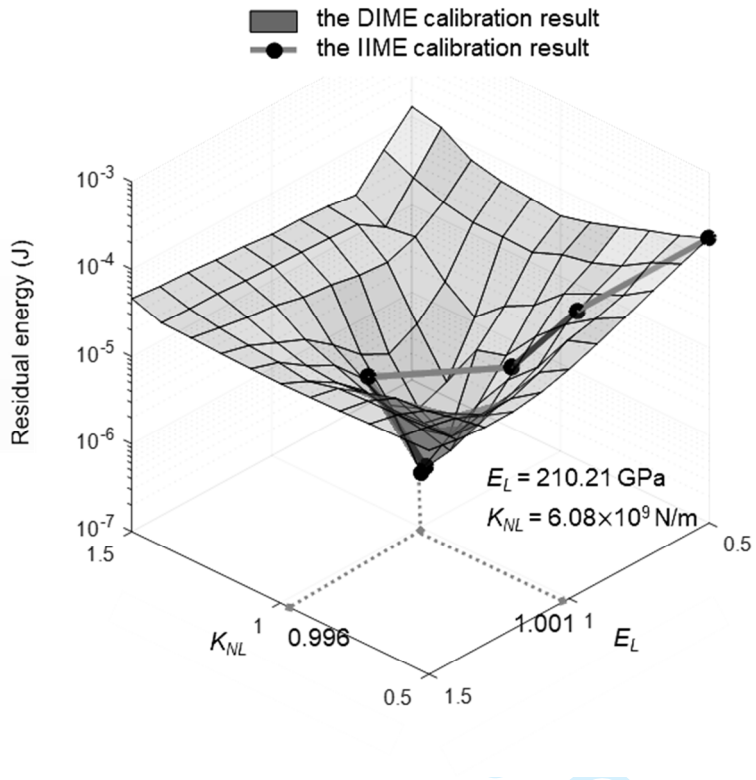

Figure 7. The calibration result for the linear and nonlinear parameters

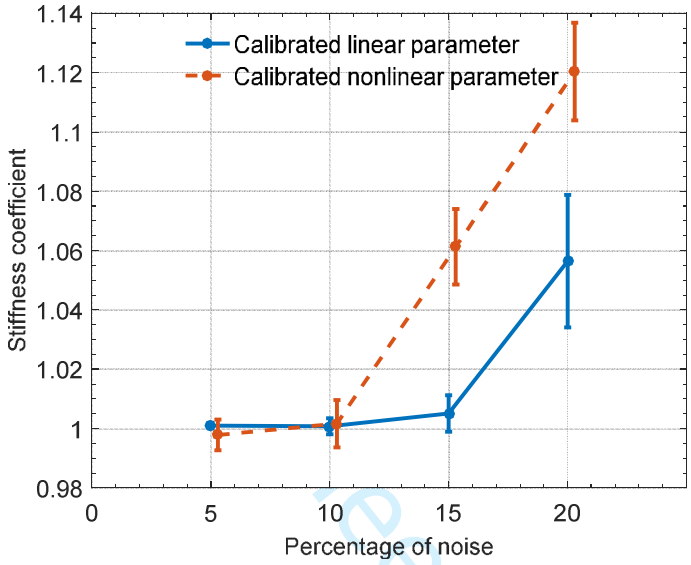

Figure 8. Mean and standard deviation error bars illustrating the calculated value of the calibrated linear and nonlinear stiffness parameters under a variety of noise levels using the proposed approach. The true values of both parameters correspond to a stiffness coefficient value of 1.

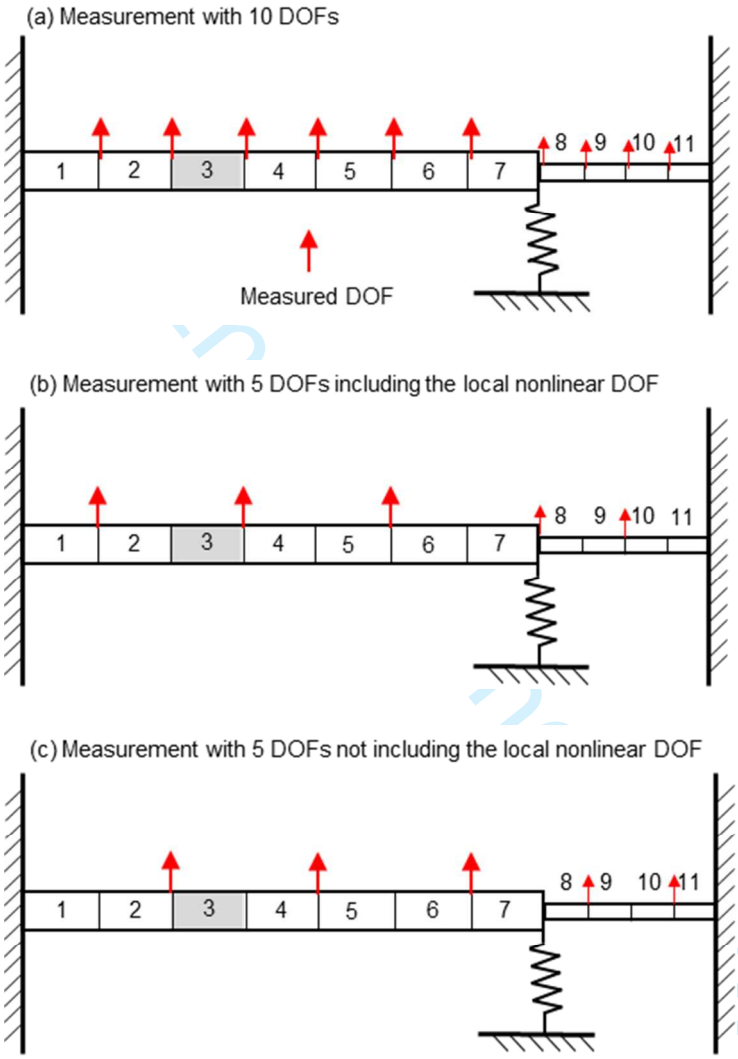

Figure 9. Three sets of reduced DOF measurements

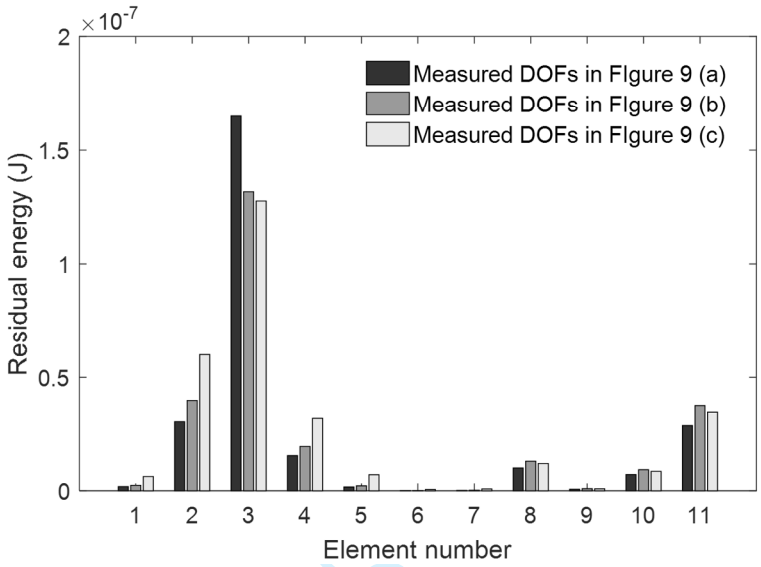

Figure 10. The ECRE localization of linear model error using reduced sets of measurements

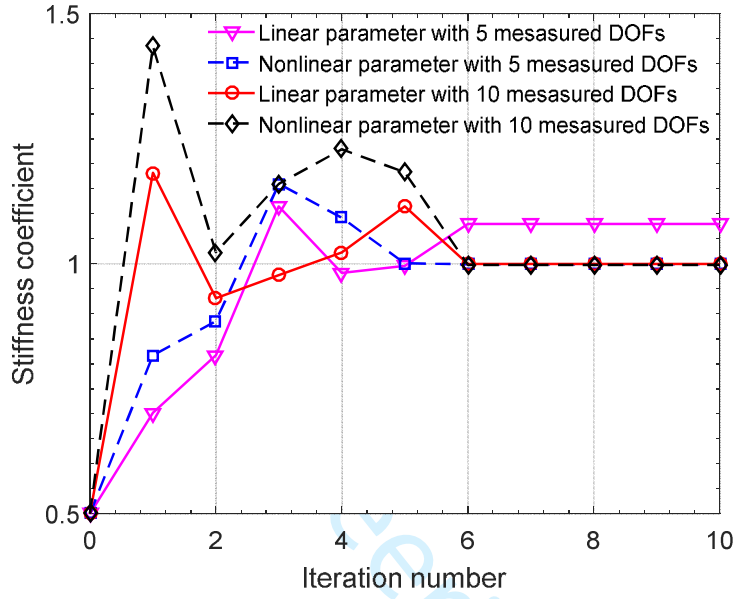

Figure 11. Calibration results with fewer measured DOFs (the nonlinear DOF is included)

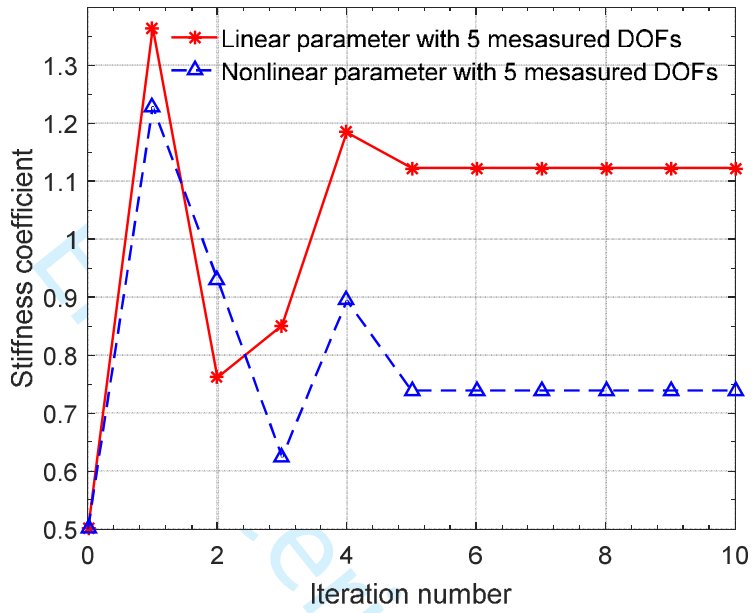

Figure 12. Calibration results with 5 measured DOFs (not including the nonlinear DOF)

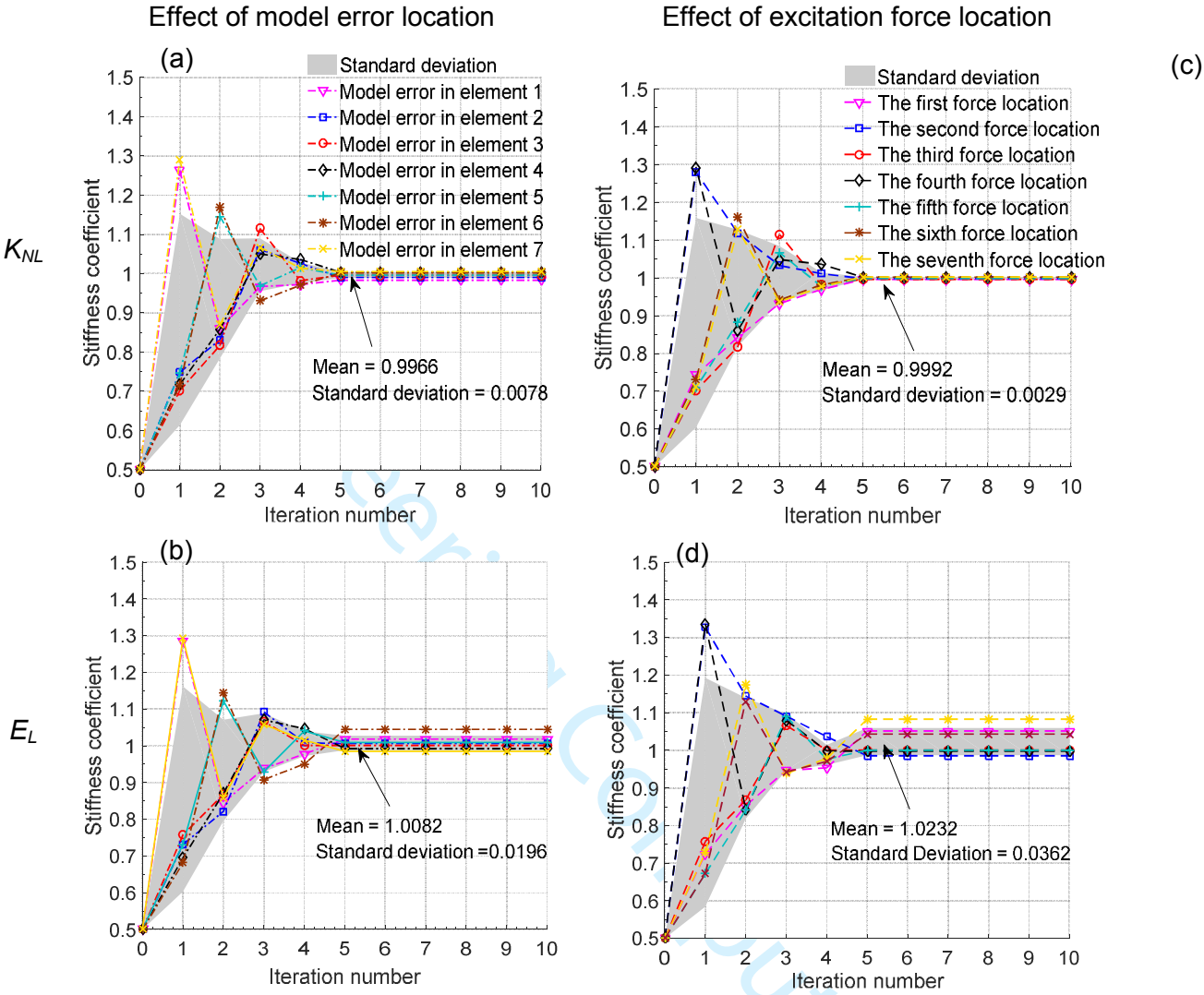

Figure 13. Calibration results considering the effect of model error location and excitation force location

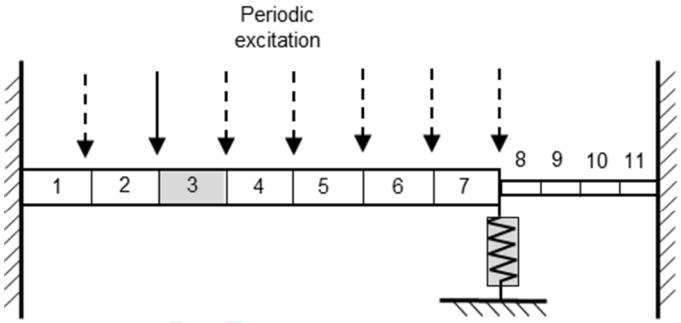

Figure 14. Seven locations for applied excitation force

Response to Reviewers' Comments

EC-10-2017-0419: Model Calibration of Locally Nonlinear Dynamical Systems: Extended Constitutive Relation Error with Multi-Harmonic Coefficients

Based on the comments provided, the authors have revised the manuscript accordingly. The authors would like to thank the reviewers for their recommendations; the authors believe they have helped to improve the paper.

Below, the comments of the reviewers are shown in black. The authors' responses are given in *blue italics.* The paragraphs modified or added in the manuscript to address the reviewer's comments are shown in *red italics*.

Comments from the Editor:

I am somewhat concerned with how similar certain sections of the paper are to the work of Isasa et al. (Model updating of locally non-linear systems based on multi-harmonic extended constitutive relation error, 2011), in particular sections 2 and 3 of the manuscript. While this paper is cited on numerous occasions throughout the manuscript, and the sections of concern are not claimed to be new material, I still found the similarity to be closer than one might normally expect. Hence I ask the authors to take this into account when revising your manuscript.

Isasa et al.'s work focused on detecting the error between a nonlinear system and its numerical model. Such modeling error may originate from the global system that exhibits the underlying linear behavior and/or the spatially local component that introduces nonlinearity. In our study, we go a step further. We not only detect the model error, but also distinguish the sources of the error (e.g. global, linear component and local, nonlinear component) and provide a framework for model calibration.

Our method consists of a two-step approach to first, under low amplitude excitation, calibrate the linear aspects of the model and then, under high amplitude excitation, identify and calibrate individual elements of the model that specifically cause error in the nonlinear response of the system. Isasa et al. do not consider model errors that may be present in the modeling of the linear components. This distinction is important because errors associated with the global, linear and local, nonlinear components, if not distinguished, may compensate and lead to misleading outcomes.

In addition, our use of an iterative approach to algorithmically identify the best values for model parameters is a significant improvement over the fact that the method of Isasa et al. is "used as an error localization indicator, and gives no explicit clues as to what model characteristics (mesh refinement, element formulation, mechanical properties, etc.) are erroneous. In practice, this is determined by trial and error." This framework for iterative and more efficient model calibration allows for improved computational cost in the effort to match finite element models to structural measurements accurately.

Comments from Reviewer #1:

1. The novelty of the manuscript and presented work is unclear. The authors need to articulate clearly the novel elements of their work/study as compared with the published literature.

Previous work focused on detecting the error between a nonlinear system and its numerical model. Such a modeling error may originate from the global system that exhibits the underlying linear behavior and/or the spatially local component that introduces nonlinearity. In our study, we go a step further. We not only detect the model error, but also distinguish the sources of the error (e.g. global, linear component and local, nonlinear component) and provide a framework for model calibration.

Our method consists of a two-step approach to first, under low amplitude excitation, calibrate the linear aspects of the model and then, under high amplitude excitation, identify and calibrate individual elements of the model that specifically cause error in the nonlinear response of the system. Published work does not consider model errors that may be present in the modeling of the linear components. This distinction is important because errors associated with the global, linear and local, nonlinear components, if not distinguished, may compensate and lead to misleading outcomes.

In addition, our use of an iterative approach to algorithmically identify the best values for model parameters is a significant improvement over methods in the published literature, which are "used as an error localization indicator, and gives no explicit clues as to what model characteristics (mesh refinement, element formulation, mechanical properties, etc.) are erroneous. In practice, this is determined by trial and error" (Isasa et al.). This framework for iterative and more efficient model calibration allows for improved computational cost in the effort to match finite element models to structural measurements accurately.

2. The submission does not include an abstract.

The online submission system appears to separate the title page (which contains the journal-specified, structured abstract and author/institution information) from the rest of the manuscript to maintain anonymity. The text of the structured abstract is included below for your review:

> **Purpose:** This paper presents an approach for calibrating the numerical models of dynamical systems that have spatially localized nonlinear components. The approach implements the Extended Constitutive Relation Error method using multi-harmonic coefficients, and is conceived to separate the errors in the representation of the global, linear and local, nonlinear components of the dynamical system through a two-step process.
>
> **Design/methodology/approach:** The first step focuses on the system's predominantly linear dynamic response under a low magnitude periodic excitation. In this step, the discrepancy between measured and predicted multi-harmonic coefficients are calculated in terms of residual energy. This residual energy is in turn used to spatially locate errors in the model, through which one can identify the erroneous model inputs which govern the linear behavior that need to be calibrated. The second step involves measuring the system's nonlinear dynamic response under a high magnitude periodic excitation. In this step, the response measurements under both low and high magnitude excitation are used to iteratively calibrate the identified linear and nonlinear input parameters.
>
> **Findings:** When model error is present in both linear and nonlinear components, the proposed Iterative Combined MHB-ECRE calibration approach has shown superiority to the conventional MHB-ECRE method, while providing more reliable calibration results of the nonlinear parameter with less dependency on a priori knowledge of the associated linear system.
>
> **Originality/value:** This two-step process is advantageous as it reduces the confounding effects of the uncertain model parameters associated with the linear and locally nonlinear components of the system.

3. What is the real-world application of the proposed method (aside from academic examples)?

This approach will hold for any problem with a local nonlinearity as part of a predominately linear system. In engineering systems, many sources of spatially localized nonlinear effects exist, including nonlinear

material behavior, second-order geometric effects, and complex boundary conditions (Gaurav et al. 2011; Shi and Atluri 1992; Fey et al. 1996), which necessitate the development, analysis, and updating of nonlinear numerical models. Local nonlinearities can also be introduced deliberately by designers to improve the engineering performance of a system by being able to avoid excessively high responses or stress (Fey 1992). One example of such applications is in rotating mechanical systems that contain nonlinear bearings, which are often modeled as structural systems with many degrees of freedom and local nonlinearities excited by periodic external loads (Yamauchi 1983; Natara and Nelson 1989). Dry friction damping elements, such as local non-linear components, have also been applied for the purpose of increasing the passive damping of various linear structural systems, such as large space structures and turbomachinery blades (Ferri and Dowell 1988). In these cases, the nonlinear effects are localized in a component of a larger system, and the main structural system remains linear for small deformations (Clough and Wilson 1979). The consistency between all of these types of systems and problems is that when the system undergoes low amplitude excitations, the linear response of the system can be isolated and calibrated independent of any influence from the nonlinear response.

The approach is presented as a two-step process in this paper. However, it can be implemented with more steps to more clearly differentiate the amplitude-dependent nonlinear responses; complicated systems could benefit from an iterative series of increasing excitations to gradually improve predominately linear and then nonlinear model accuracy.

The presented approach can also be applied to problems with nonlinear elements that are not necessarily confined in a local, geometric region. Once low amplitude excitations allow the analysis and calibration of the linear system parameters, increasingly higher excitation(s) can draw out the nonlinear response for subsequent calibration. This segmented approach can be applied to all nonlinear dynamics problems; the particular equations (equilibrium equations, etc.) would need to be revisited.

4. How can this approach be applied to other nonlinear dynamic systems, aside from geometrically nonlinear systems as shown in Eq. 3?

The nonlinear system does not necessarily need to be a geometrically (or even locally) nonlinear system. The only requirement is proper parameterization to describe a property of the elements in the structural model that, when calibrated, can reduce the residual error between the model predictions and the experimental measurements. This parameterized property could represent any number of aspects of a finite element model, such as the stiffness coefficients, mass, density, etc., that describe the nonlinear behavior of the actual system. The response to Question 3 above presents several real-world cases where this approach could be applied to designed systems. In all of these cases, a representative finite element model of the system would contain parameters to represent these components that introduce nonlinear response and could be calibrated using the proposed method.

An additional explanation to this effect has been added to Section 2:

A local, cubic nonlinearity is used in this paper as it is one of the most common cases of nonlinearity in dynamic systems (Kerschen et al. 2006; Wilson et al. 1972). It is important to note, however, the approach presented herein can be used for a wide variety of nonlinear systems (not just local nonlinearities) where the underlying system can be analyzed and calibrated first using intentionally low excitations to the system to isolate the predominately linear behavior of the system (Stricklin and Haisler 1977).

5. How the term $\mathbf{x}^3$ is defined in Eq. 1, where $\mathbf{x}$ is a Nx1 vector?

The term $\boldsymbol{x}^3$ is defined as an element-wise power applied to each element of the vector (cubing the displacement of each DOF of the system). The explanation of that equation has been similarly clarified.

"In Equation (1), a spatially localized, geometrical nonlinearity is represented by the cubic stiffness, K_{NL}, multiplied by the element-wise cube of the displacement of each DOF (Worden and Tomlinson 2000)."

6. Please provide a reference for Eq. 4.

The reference for that equation formulation is (Isasa et al. 2011) and has been added to the manuscript accordingly.

"…following frequency domain expression can be obtained (Isasa et al. 2011):

$$\mathcal{Z}(\omega)\boldsymbol{Q}_\omega + \boldsymbol{F}(\boldsymbol{Q}_\omega, \omega) - \boldsymbol{P} = 0 \qquad (4)"$$

7. What is the "constitutive error of the system" on page 7, line 50?

The constitutive relation error (CRE) of the system is an element-wise measure of the residual energy due to the discrepancy between model predictions and the structure (Charbonnel et al. 2013; Deraemaeker et al. 2002; Ladevèze and Leguillon 1983). These discrepancies are commonly calculated based on constitutive relations of the structure or material, such as the relationship between elemental stress and strain or the multi-harmonic coefficients described in this paper.

This method was developed into the "extended constitutive relation error" (ECRE) as a way to provide a framework for the use of CRE for not only error detection, but also model improvement. This expansion integrates the mechanistic principles (e.g. load-displacement relationships) underlying the behavior of the system during the comparison of model predictions against experiments (Chouaki et al. 1998; Hu et al. 2017; Ladevève et al. 1999). This expansion then allows for pinpointing the elemental contributions to the total error considering both model and experimental errors.

This explanation has been added to the introduction to aid in understanding of this topic, along with the cited references.

"When coupled with the extended constitutive relation error (ECRE), a method to measure the element-wise discrepancy between a model and a structure based on constitutive relations, the multi-harmonic coefficients allow the calculation of the residual energy that reflects the discrepancy between predictions and measurements (Charbonnel et al. 2013; Deraemaeker et al. 2002; Hu et al. 2017; Ladevèze and Leguillon 1983).

8. On page 8, line 39, how $\mathbf{K}_R$ is obtained through mode reduction?

The term $\boldsymbol{K}_R$ is obtained through model reduction using the Guyan reduction technique (Guyan 1965). This clarification has been added to the manuscript. More specifically, the Guyan model reduction technique is applied to each stiffness matrix (N by N) in Equation (9). Then, the reduced stiffness matrix (N_e by N_e) is reassembled into the multi-harmonic stiffness matrix with a resulting dimension of ($(2n+1)N_e$ by $(2n+1)N_e$).

Finally, $\mathcal{K}_R$ is the $(2n+1)N_e \times (2n+1)N_e$ reduced multi-harmonic stiffness matrix of the numerical model obtained by Guyan model reduction, where N_e is the number of measured DOFs.

9. The reviewer could not follow Eq. 12.

The minimization problem that results in Equation 12 can be considered a saddle-point problem that can then be formulated with the introduction of Lagrange multipliers. The cost function for a specific value of P_1 is as follows, and it is this specific error that the approach seeks to minimize:

$$E_{\omega 1}^2 = r_{\omega 1}^T \mathcal{K} r_{\omega 1} + \alpha (HQ_{\omega 1} - Q_{\omega 1}^e)^T \mathcal{K}_R (HQ_{\omega 1} - Q_{\omega 1}^e)$$

The terms that compose this equation are classified as being "less reliable," namely the error in the model (first term) and the mode shape expansion error (second term) that is introduced when the experimentally measured information is extrapolated to the N model DOFs (Zimmerman and Kaouk 1994). By subsequently applying the constraint to the optimization problem that the solution must satisfy the more reliable equilibrium equation, the errors in less reliable equations can be minimized. This constraint equation is shown below:

$$Z(\omega) Q_{\omega 1} + F(Q_{\omega 1}, \omega, K_{NL}) - P_1 = \mathcal{K} r_{\omega 1}$$

Table 1 below presents several common equations that may be considered reliable or less reliable in numerical models and experimental measurements (Charbonnel et al. 2013; Deraemaeker et al. 2002).

Table 1: Common reliable and less reliable equations

	Numerical Model	*Experimental Campaign*
Reliable Equations and Quantities	*Geometric Information* *Kinematic Equations* *Equilibrium Equations*	*Measured Natural Frequencies* *Sensor Locations and Directions* *Excitation Force Locations and Directions*
Less Reliable Equations and Quantities	*Constitutive Equations*	*Measured Mode Shapes*

Through the use of Lagrange multipliers, the optimization function and the constraint can be incorporated into the single minimization function h below, where the vector λ represents the Lagrange multipliers.

$$h = r_{\omega 1}^T \mathcal{K} r_{\omega 1} + \alpha (HQ_{\omega 1} - Q_{\omega 1}^e)^T \mathcal{K}_R (HQ_{\omega 1} - Q_{\omega 1}^e) + \lambda^T (\mathcal{K} r_{\omega 1} - Z(\omega) Q_{\omega 1} - F(Q_{\omega 1}, \omega, K_{NL}) + P_1)$$

Finally, by taking the derivative of h with respect to r_w, $Q_{\omega 1}$, and λ and setting those equations equal to zero, h can be rewritten as the following system of nonlinear equation to solve:

$$\begin{pmatrix} Z(\omega) + \dfrac{\partial F(Q_{w1}, \omega)}{\partial Q_{w1}} & \alpha H^T \mathcal{K}_R H \\ \mathcal{K} & -Z(\omega) \end{pmatrix} \begin{Bmatrix} r_{w1} \\ Q_{w1} \end{Bmatrix} + \begin{Bmatrix} 0 \\ -F(Q_{w1}, \omega) \end{Bmatrix} = \begin{Bmatrix} \alpha H^T \mathcal{K}_R Q_{w1}^e \\ -P_1 \end{Bmatrix}$$

Comments from Reviewer #2:

1. While the method is tested for a simple problem with relatively few degrees of freedom, could the authors comment on how the computational cost would be expected to scale as the number of degrees of freedom increases?

As the number of degrees of freedom increases, the size of the stiffness and mass matrices, as well as the potential number of parameters to calibrate, would increase. Thus, it is expected that the computational cost would also increase. However, since the computational cost strongly depends on the number of parameters to calibrate and the effect of increased size of the nonlinear equation matrix, the authors are unaware of an approach that can predict how the computational cost would increase when the proposed method is applied to a more complex problem. While work has been done to try and predict the convergence of nonlinear systems of equations (Guo 2011; Lin et al. 2010), the equations to solve would depend on the system in question and its particular form of nonlinearity.

The authors would also like to highlight that the proposed iterative optimization in the model calibration process, compared to the discrete approach utilized in previous literature (Silva et al. 2008; Isasa et al. 2011), can significantly reduce the computational cost by achieving an optimal solution (closest to the true parameter value) with a far fewer number of iterations.

2. Could the authors comment further on the types of nonlinear systems for which this method should be expected to work? For example, are there nonlinear systems for which harmonic responses at only two amplitudes would be insufficient?

The method would be expected to work on a wide array of nonlinear systems, not necessarily just geometrically nonlinear systems. The only requirement is proper parameterization to describe a property of the elements in the structural model that, when calibrated, can reduce the residual error between the model predictions and the experimental measurements. This parameterized property could represent any number of aspects of a finite element model, such as the stiffness coefficients, mass, density, etc., that describe the nonlinear behavior of the actual system. In the response to Reviewer #1 above, several common, real-world engineering applications are presented to which this method can be applied.

A natural extension of this approach is increasing the applied excitation in a gradual manner and evaluating the residual energy between the model predictions and the experimental measurements to assess the error that can be minimized through calibration of the parameters that control the nonlinear behavior. This extension would expand the proposed approach from a "two-step" method to an iterative, multi-step approach. The authors believe that complicated systems could benefit from this iterative series of increasing excitations to gradually improve the predominately linear and then nonlinear model accuracy if the two responses cannot be clearly distinguished from one another with a single excitation step. This is certainly an area of further research in the development of a more universally-applicable framework for nonlinear system identification and calibration.

This further explanation has been added to the conclusion as an area for further work in improving the robustness and applicability of this approach:

"One area for further work includes the natural extension of this approach in increasing the applied excitation in a gradual manner and assessing the residual energy between model predictions and the experimental measurements. This extension would expand the proposed approach from a "two-step" method to an iterative, multi-step approach. The authors believe that complicated systems could benefit from this iterative series of increasing excitations to gradually improve the predominately linear and then

nonlinear model accuracy if the two responses cannot be clearly distinguished from one another with a single excitation step. This is certainly an area of further research in the development of a more universally-applicable framework for nonlinear system identification and calibration."

3. Section 2.1: starts with an example of a very specific form of nonlinearity. It might be better to start with a more general nonlinear system, so that the readers are not given the impression that the present method should only work for cubic nonlinearities of the form given here.

The local, cubic nonlinearity presented is this paper was chosen for being one of the most common cases of nonlinearity in dynamic systems (Kerschen et al. 2006; Wilson et al. 1972). The approach, however, can be used for any nonlinear system (not necessarily just local nonlinearities) where the underlying linear system can be analyzed and calibrated first using intentionally low excitations to the system (Stricklin and Haisler 1977).

The authors thank the reviewer for this advice and have included an explanation of the applicability of this method to other nonlinear systems into the paper:

"A local, cubic nonlinearity is used in this paper as it is one of the most common cases of nonlinearity in dynamic systems (Kerschen et al. 2006; Wilson et al. 1972). It is important to note, however, the approach presented herein can be used for a wide variety of nonlinear systems (not just local nonlinearities) where the underlying system can be analyzed and calibrated first using intentionally low excitations to the system to isolate the predominately linear behavior of the system (Stricklin and Haisler 1977)."

4. In equations 6 and 7, should m_1 be inside the sine and cosine functions?

Yes, those equations should be corrected as you suggested. Both have been adjusted and below is the corrected version of Equation 6:

$$\boldsymbol{F}(\boldsymbol{Q}_{\omega},\omega)=\begin{Bmatrix}\int_0^T f_{NL}(\boldsymbol{x}(t))dt\\ \frac{\omega}{\pi}\int_0^T f_{NL}(\boldsymbol{x}(t))\cos m_1\omega t dt\\ \frac{\omega}{\pi}\int_0^T f_{NL}(\boldsymbol{x}(t))\sin m_1\omega t dt\\ \vdots\\ \frac{\omega}{\pi}\int_0^T f_{NL}(\boldsymbol{x}(t))\cos m_n\omega t dt\\ \frac{\omega}{\pi}\int_0^T f_{NL}(\boldsymbol{x}(t))\sin m_n\omega t dt\end{Bmatrix}$$

5. It is interesting that figure 8 seems to show a bias error in the estimation of the stiffness coefficients due to noise (i.e., noisy data seems to give an overestimation of the stiffness). Could the authors comment on this phenomenon, and its implications for using this method to obtain accurate parameter estimates from noisy data? The authors comment in the conclusion that "These studies show that the method is quite robust against introduced measurement noise", but this plot seems to indicate that, for certain noise levels, even taking the average over multiple trials will not give an accurate estimate of the parameters, no matter how many

trials/noise realizations are taken. Perhaps it should also be reemphasized in the caption of figure 8 that the error bars are based on the variance across multiple noise realizations, rather than representing an accurate estimate of the range that the true value could take based on measurements (if the latter were the case, then one would expect the error bars to include the true stiffness values).

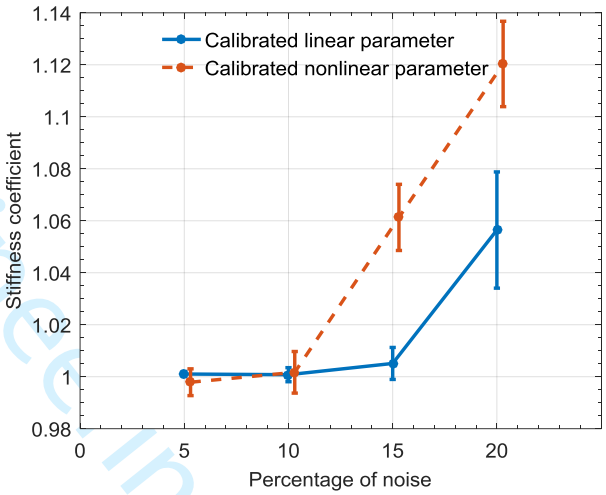

Figure 8. Mean and standard deviation error bars illustrating the calculated value of the calibrated linear and nonlinear stiffness parameters under a variety of noise levels using the proposed approach. The true value of both parameters correspond to a stiffness coefficient value of 1.

For each noise level, 10 random realizations of noise are generated to contaminate the time history data and, subsequently, 10 sets of calibrated model parameters are obtained using the contaminated measurements. The error bars in Figure 8 illustrate the standard deviation around the mean of the obtained 10 sets of calibrated parameters.

Using the contaminated measurements, it is expected that the calibrated parameters would deviate from the true stiffness values. This is because the proposed method is searching for a set of parameters that minimize the residual energy between the numerical model and the physical structure. When the introduced measurement noise is significant enough, it can become another source of the calculated residual energy that the approach will attempt to account for using the calibration parameters, and thus affect their calculated values (Hu et al. 2017).

The proposed approach can achieve less than 1% error in the calibrated nonlinear parameter when the random noise level is set to 10%, and less than 1% error in the calibrated linear parameter when the noise level is at 15%. The authors believe these introduced noise levels are high enough to verify the proposed method's robustness against measurement noise. The objective of including higher noise levels (15-20%) is to further test the capability of the proposed method. Even at 20% noise, the calibrated nonlinear stiffness is varied only approximately 12% from an original error of 50%.

The caption for Figure 8 has been clarified using the reviewer's suggestion.

6. In Section 5.2, the paper by Majumder and Manohar (2003) is referred to, but it does not appear in the reference section.

We thank the reviewers for pointing out this omission. This reference has been added to the reference section in the appropriate location.

Majumder, L., Manohar, C.S. (2003). A time-domain approach for damage detection in beam structures using vibration data with a moving oscillator as an excitation source. Journal of Sound and Vibration, 268*(6), 699-716.*

REFERENCES:

Charbonnel, P. E., Ladevèze, P., Louf, F., & Le Noac'h, C. (2013). A robust CRE-based approach for model updating using in situ measurements. *Computers & Structures*, *129*, 63-73.

Chouaki, A. T., Ladevèze, P., & Proslier, L. (1998). Updating structural dynamic models with emphasis on the damping properties. *AIAA Journal*, *36*(6), 1094-1099.

Deraemaeker, A., Ladevèze, P., & Leconte, P. (2002). Reduced bases for model updating in structural dynamics based on constitutive relation error. *Computer methods in applied mechanics and engineering*, *191*(21), 2427-2444.

Guo, C. H., (2001). Convergence rate of an iterative method for a nonlinear matrix equation. *SIAM Journal on Matrix Analysis and Applications*. *23*(1), 295-302.

Guyan, R. J. (1965). Reduction of stiffness and mass matrices. *AIAA Journal*, *3*(2), 380.

Hu, X., Prabhu, S., Atamturktur, S., & Cogan, S. (2017). Mechanistically-informed damage detection using dynamic measurements: Extended constitutive relation error. *Mechanical Systems and Signal Processing*. 85, 312-328.

Kerschen, G., Worden, K., Vakakis, A. F., & Golinval, J. C. (2006). Past, present and future of nonlinear system identification in structural dynamics. *Mechanical Systems and Signal Processing*, *20*(3), 505-592.

Ladevèze, P. & Leguillon, D. (1983). Error Estimate Procedure in the Finite Element Method and Applications. *SIAM J. Numer. Anal.*, *20*(3), 485-509.

Ladavèze, P., Moës, N., & Douchin, B. (1999). Constitutive relation error estimators for (visco)plastic finite element analysis with softening. *Computer Methods in Applied Mechanics and Engineering*, *176*(1-4), 247-264.

Lin, Y., Bao, L., & Jia, X. (2010). Convergence analysis of a variant of the Newton method for solving nonlinear equations. *Computers & Mathematics with Applications*, *59*(6), 2121-2127.

Stricklin, J. A. & Haisler, W. E. (1977). Formulations and solution procedures for nonlinear structural analysis. *Computers & Structures*, 7, 125-136.

Wilson, E. L., Farhoomand, I., & Bathe, K. J. (1972). Nonlinear dynamic analysis of complex structures. *Earthquake Engineering & Structural Dynamics*, *1*(3), 241-252.

Zimmerman, D.C. & Kaouk, M. (1994). Structural damage detection using minimum rank update theory. *J. Vib. Acoust.*, *116*(2), 222-231.